PROPAGATION CHARACTERISTICS OF MICROSTRIP TRANSMISSION LINES

PROPAGATION CHARACTERISTICS OF MICROSTRIP TRANSMISSION LINES ON INTRINSIC GERMANIUM SUBSTRATES

By

MAGID YOUSRI DIMYAN, B.Sc.

A Thesis
Submitted to the Faculty of Graduate Studies
in Partial Fulfilment of the Requirements
for the Degree
Master of Engineering

McMaster University
January 1969

MASTER OF ENGINEERING (1969)
(Electrical Engineering)

McMASTER UNIVERSITY
Hamilton, Ontario

TITLE: Propagation Characteristics of Microstrip Transmission Lines on Intrinsic Germanium Substrates

AUTHOR: Magid Yousri Dimyan, B.Sc. (Cairo University, Giza, Egypt)

SUPERVISOR: Professors M. W. Gunn and S. H. Chisholm

NUMBER OF PAGES: 98, IX

SCOPE AND CONTENTS:

The propagation characteristics of microstrip transmission lines are theoretically analysed using both conformal transformation and variational techniques.

A method for measuring the characteristic impedance of microstrip lines through a lossy junction using a high precision reflection bridge is described.

Microstrip lines on intrinsic germanium substrates were built in the laboratory and their characteristic impedance measured at a frequency of 9.38 GHz.

ABSTRACT

The microstrip transmission line has been theoretically analysed using conformal transformation and variational techniques. The variational method has been used to compute the line capacitance, characteristic impedance and guide wavelength of the following microstrip structures:

(i) Microstrip transmission lines having negligible and finite strip conductor thickness.

(ii) Microstrip transmission lines on two layer dielectric substrates having negligible and finite strip conductor thickness.

The total losses incurred in microstrip lines on semiconductor substrates have been included. An experimental technique (based on the Deschamps method) for measuring the characteristic impedance of microstrip lines through a lossy junction using a high precision microwave reflection bridge has been described. Measurements of the characteristic impedance of microstrip lines on intrinsic germanium substrates have been carried out at 9.38 GHz, and good agreement between the theoretical and experimental results have been obtained.

ACKNOWLEDGEMENTS

The author wishes to express his sincere gratitude to Professors M. W. Gunn and S. H. Chisholm for their helpful advice and criticism during the course of this work. Thanks are also due to Professor C. K. Campbell for the use of the Edwards High Vacuum coating unit.

TABLE OF CONTENTS

LIST OF FIGURES

LIST OF TABLES

CHAPTER I

INTRODUCTION

1.1 MICROWAVE INTEGRATED CIRCUITS:

A microwave integrated circuit (I.C.) can be defined to be a subsystem or function comprising a miniaturized planar circuit of solid state devices[1]. Switches, amplifiers, mixers, harmonic generators, filters, oscillators, phase shifters, lumped elements, combination transmit-receive switches, etc. have been successfully built as I.C.'s and the list continues to grow.

Like all I.C.'s, microwave integrated circuits prove to have higher reliability, greater versatility, smaller size and weight and lower production cost than conventional circuitry. However, all the integrated circuits built so far are for applications that do not require high power at high frequencies. And as yet, the complexity of design and fabrication techniques of such circuits have not been completely resolved. In general, microwave I.C.'s may be in one of the following forms: -

(a) Hybrid - in which semiconductor active chip devices serving as transistors and diodes are attached to ceramic substrates by either parallel gap welding, ultrasonic bonding or thermocompression bonding. The passive devices are deposited by thick or thin film processing techniques.

(b) Monolithic - in which the substrates are high resistivity (usually over 1000 Ω-cm) semiconductor. Both Silicon and Gallium Arsenide have been successfully used. Active elements such as diodes and transistors are formed by diffusions in the epitaxial crystal. Passive elements such as resistors and capacitors may be diffused into the epitaxial layer or substrate or deposited along with inductors as thin films on either an epitaxial layer or the substrate.

(c) Silicon-on-Sapphire - in which films of silicon are deposited on sapphire substrates to form isolated active devices by etching and diffusing the film.

1.2 MICROSTRIP:

Microstrip is a major element in the design of microwave I.C.'s. It is not only required for matched interconnections (microstrip transmission lines), but also in the design of such circuit elements as filters, impedance matching networks, attenuators, resonators, etc.

A microstrip transmission line consists of: -

(a) A thin conductor strip of width w and thickness t.

(b) A substrate of thickness h - which may be a high resistivity semiconductor, a low loss ceramic dielectric, a high permittivity ($\varepsilon_r > 100$) dielectric, etc.

In the case of the semiconductor substrate, a thin film of SiO or SiO_2 is sometimes used to insulate the substrate from the strip conductor.

(c) A metallized ground plane - which forms a common ground plane for the transmission system. Its presence facilitates heat transfer as well as reduces the noise coupling between neighbouring lines.

Because of fringe field and radiation problems which exist with microstrip lines, the Triplate or Strip-line structure using two ground planes to confine the fringe field has been frequently used in the design of conventional microwave circuits. However, because the microstrip line has a nearly planar structure, it is now being extensively employed in microwave integrated circuits. Fortunately, with high permittivity substrates, the fields stay close to the strip conductor, and the radiation problems are considerably reduced.

Since in a microstrip line part of the field is contained in the dielectric medium and part in the air above the conductor, the structure is inhomogeneous with respect to the field parameters and hence cannot support a TEM mode. The resulting mode is termed a quasi - TEM mode, and it has been shown[11,13] that the error incurred in assuming it to be a pure TEM mode is negligible.

1.3 HISTORY OF MICROSTRIP:

Microstrip Transmission Lines were developed at the Federal Telecommunications Laboratories, Inc., N.J. as a substitute for waveguides or coaxial lines. They first received prominence when three papers were published simultaneously in the Proceedings of the IRE in December 1952. In one of these papers Assadourian and Rimai[2] outlined a simplified theory for microstrip lines based on the assumption of TEM propagation. However, their theory proved to be only accurate for "wide" lines, i.e. for lines of strip width/substrate thickness > 2. The other two papers published in the same issue[3,4] gave design and structural details of microstrip lines on such low permittivity substrates as polystyrene, fiberglas, teflon, formica, etc.

The interest in microstrips in the early 195o's culminated in a special issue of the IRE Trans. on Microwave Theory and Techniques in

March 1955. In this issue, J. Arditi published a paper on the measurement of microstrip line properties through a lossy microstrip to coaxial transducer by using the Deschamps method[5]. This was an extension of a previous paper[6].

In the same issue of the MTT, Black and Higgins presented their rigorous solution of the parameters of microstrips[7], but unfortunately their solution was good only for the case of an infinite and uniform dielectric media, i.e. for microstrip lines with air dielectric.

In 1956, Dukes measured the properties of microstrips using an electrolytic tank[8], and noted that the losses predicted by Assadourian and Rimai[2] were higher than those actually observed.

In 1957, Wu[9] outlined a procedure which accounts for the fringing electrostatic fields, dielectric discountinuity and radiation losses incurred in microstrip lines, but his solution proved to be too complex, and general design curves for microstrip components were not feasible.

Perhaps the greatest breakthrough in the theoretical analysis of microstrip lines came in 1965 when H. A. Wheeler published his now classical conformal-mapping approximation solution[10,11] in which he assumed a TEM propagation and accounted for the dielectric discountinuity. M. Caulton et al[12], working on microstrip lines on ceramic substrates, and using approximate measurement techniques have concluded that Wheeler's solution was reasonably accurate and have extracted a set of design curves for use with microstrip lines on any substrate. R. Seckelmann, using a newly developed nodal shift method for measuring microstrip properties[13] also obtained experimental data[14], which agreed fairly accurately with the theoretical results based on Wheeler's analysis.

The first experimental work on Microstrips on Semiconductor substrates was carried out in 1965 by T. M. Hyltin[15]. The method he used was based on that described by J. Arditi[6], but the electrical length of the transmission line was changed by changing the frequency. This technique is similar to that described by H. Lenzing[16].

In 1965, H. Green[17], employing highly advanced over-relaxtion techniques in solving Laplace's equation using a digital computer, obtained a numerical solution for the characteristic impedance and velocity ratio of microstrip lines. K. Wolters and P. Clar[18] using the same numerical technique obtained solutions for microstrips on very high dielectric constant substrates such as titanium diode/magnesium oxide ceramic.

Cuckel et al[19] using a parallel plate waveguide approach on microstrip lines on silicon substrates, obtained a series of design curves which establish qualitative data for substrate conductivities.

However, the most recent and perhaps simplest method for the analysis of microstrip lines was that proposed by E. Yamashita and R. Mittra[20], and which will be fully investigated in this thesis.

1.4 OUTLINE OF THE THESIS:

This thesis describes two methods for analyzing microstrip transmission lines. The first method is based on a Schwarz-Christoffel conformal transformation, and a semi-infinite parallel plate structure is first considered. The capacitance of such a structure can be computed by solving numerically two transcendental equations using the Newton-Raphson method. By a simple analogy, the capacitance and hence the characteristic impedance of a microstrip line of strip width W and substrate thickness h can be obtained.

The second method of microstrip analysis is based on the application of Fourier transform and variational techniques. The following microstrip structures are considered: -

(a) Microstrip transmission lines having negligible and finite strip conductor thickness.

(b) Microstrip transmission lines on two-layer dielectric substrates having negligible and finite conductor thickness.

Design charts are provided for intrinsic Germanium ($\varepsilon_r = 16.0$)[21] substrates in case (a) above and for intrinsic Germanium and Si_3N_4 or $A\ell_2 0_3$ ($\varepsilon_r \approx 7.0$) substrates in case (b).

A method for measuring the characteristic impedance of microstrip transmission lines based on the Deschamps method is described.

An experimental verification of the characteristic impedance was performed on microstrip lines on intrinsic Germanium substrates at 9.38 GHz using a reflection type microwave bridge.

CHAPTER II

THEORETICAL ANALYSIS

2.1 CHARACTERISTIC IMPEDANCE OF MICROSTRIP TRANSMISSION LINES USING THE SCHWARZ-CHRISTOFFEL TRANSFORMATION:

This method gives approximate results for the characteristic impedance of microstrip lines. However fairly good results are obtained for values of $W/h > 0.6$, i.e. for values of $Z_o < 50$ ohms using Ge substrates ($\varepsilon_r = 16.0$).

In order to determine the characteristic impedance of microstrip lines using this method, a semi-infinite parallel-plate capacitor of plate separation d and negligible plate thickness will first be considered (see Figure 2.1, p. 13).

To obtain the capacitor boundaries in the complex W plane, the points W_1 and W_3 will in the limit be at $-\infty$ (see Figure 2.2, p. 13).

In the limit, the external angles at W_1, W_2, W_3, and W_4 will be $-\pi$, $-\pi$, π, and $-\pi$ radians respectively.

If the points W_1, W_2, W_3 and W_4 in the complex W plane map into the points x_1, x_2, x_3, and x_4 in the Z plane, then the required Schwarz-Christoffel transformation is of the form:

$$W(Z) = A_1 \int^{Z} (Z-x_1)^{-\pi/\phi_1} (Z-x_2)^{-\pi/\phi_2} (Z-x_3)^{-\pi/\phi_3} (Z-x_4)^{-\pi/\phi_4} dZ + B \qquad (2.1)$$

where A_1 = a constant serving to rotate and magnify the figure in the W plane,

B = a constant serving to translate the figure in the W plane, and

$$\phi_1 = -\pi, \quad \phi_2 = -\pi, \quad \phi_3 = \pi, \quad \text{and } \phi_4 = -\pi$$

$$\therefore\ W(Z) = A_1 \int^Z (Z-x_1)(Z-x_2)(Z-x_3)^{-1}(Z-x_4)dZ + B$$

$$= A \int^Z (1 - \frac{Z}{x_1})(Z-x_2)(Z-x_3)^{-1}(Z-x_4)dZ + B \qquad (2.2)$$

where $A = A_1 x_1$.

In order to cover the whole x-axis, let x_1 tend to ∞. Choosing $x_2 = 1$, $x_3 = 0$, and $x_4 = 1$, then by substituting in equation (2.2), one gets:

$$W(Z) = A \int^Z (Z+1)\,\frac{1}{Z}\,(Z-1)dZ + B$$

$$= A \int^Z \frac{(Z^2-1)}{Z}\,dZ + B$$

or

$$W(Z) = A[\,\frac{Z^2}{2} - \ln(Z)\,] + B \qquad (2.3)$$

Boundary Conditions -

$$\left.\begin{array}{lll} (1) & Z = -1 & \text{when } W = jd \\ & Z = 1 & \text{when } W = 0 \end{array}\right\} \text{-------------} \quad (2.4)$$

Substituting for the boundary conditions in equation (2.3) gives:

$$\left.\begin{array}{l} A(\frac{1}{2} - j\pi) + B = jd \\ \frac{1}{2}A + B = 0 \end{array}\right\} \text{-------------} \quad (2.5)$$

Solving for A and B gives $A = -\frac{d}{\pi}$, and $B = \frac{d}{2\pi}$. Therefore by substituting for A and B in equation (2.3), the mapping function will be given by:

$$W(Z) = \frac{d}{\pi} \left(\frac{1-Z^2}{2} + \ln(Z) \right) \tag{2.6}$$

The conformed mapping of the capacitor boundaries into the Z plane is depicted in Figure 2.3. The positive x-axis has a potential of zero and represents the bottom plate in the W plane, while the negative x-axis has a potential of V_o and represents the upper plate.

At any point in the x-y plane, the potential will be given by:

$$= V_o \frac{\theta}{\pi} = \frac{V_o}{\pi} \tan^{-1} (y/x) \tag{2.7}$$

By Gauss' Law, the charge density on the plane $x < 0$ is given by:

$$\rho_s\Big]_{x<0} = -\varepsilon_o \frac{\partial\phi}{\partial n} = \varepsilon_o \frac{1}{r} \frac{\partial\phi}{\partial\theta}$$

$$\rho_s\Big]_{x<0} = \frac{\varepsilon_o V_o}{|x| \pi} \tag{2.8}$$

Similarly, the charge density on the plane x · 0 will be given by: -

$$\rho_s\Big]_{x>0} = \frac{-\varepsilon_o V_o}{|x| \pi} \tag{2.9}$$

In the practical case, let the width of the parallel-plate capacitor be ℓ, the plate spacing d and the relative dielectric constant of the medium between the plates ε_r.

If the thickness of the plates is negligibly small, then when $W = -\ell$ on the inside of the lower plate, let $x = X_1$ in the Z plane where $0 < X_1 < 1$. Also, when $W = -\ell$ on the outside of the lower plate, let $x = X_2$ in the Z-plane, where $X_2 > 1$.

$\therefore$ the total charge per plate $Q = \int_{X_1}^{X_2} \rho_s \, dx$

or

$$Q = \frac{\varepsilon_o \varepsilon_r V_o}{\pi} \int_{X_1}^{X_2} \frac{dx}{x}$$

$$\therefore \quad Q = \frac{\varepsilon_o \varepsilon_r V_o}{\pi} \ln \left(\frac{X_2}{X_1}\right) \tag{2.10}$$

and

$$C = Q/V_o = \frac{\varepsilon_o \varepsilon_r}{\pi} \ln \left(\frac{X_2}{X_1}\right) \tag{2.11}$$

where X_1 and X_2 are the solutions of the two equations:

$$\frac{-\pi \ell}{d} = \frac{1 - X_1^2}{2} + \ln (X_1) \qquad 0 < X_1 < 1 \tag{2.12}$$

and

$$\frac{-\pi \ell}{d} = \frac{1 - X_2^2}{2} + \ln (X_2) \qquad X_2 > 1 \tag{2.13}$$

The two transcendental equations (2.12) and (2.13) can be numerically solved by means of a digital computer using the Newton-Raphson method.

The characteristic impedance of a parallel plate capacitor of total width = 2ℓ (see Figure 2.4) will be:

$$Z_o = \sqrt{\frac{\mu_o \varepsilon_o \varepsilon_r}{2C}}$$

Substituting for C from equation (2.11) gives:

$$Z_o = \frac{\sqrt{\mu_o / \varepsilon_o}}{\frac{2\sqrt{\varepsilon_r}}{\pi} \ln \left(\frac{X_2}{X_1}\right)} \tag{2.14}$$

where X_1 and X_2 are the solutions of equations (2.12) and (2.13).

Shown in Figure 2.5 is a comparison between the parallel-plane guide (which is approximately equivalent to a parallel-plate capacitor) and the microstrip transmission line with strip width W and substrate thickness h. Using the theory of images, both structures are equivalent when $h = d/2$, $W = 2\ell$, and $[Z_o]_{microstrip} = \frac{1}{2}[Z_o]_{parallel\ plane}$.

It immediately follows that the characteristic impedance of the microstrip line will approximately be given by:

$$Z_o = \frac{\frac{1}{2}\sqrt{\mu_o/\varepsilon_o}}{\frac{2\sqrt{\varepsilon_r}}{\pi}\ \ln\left(\frac{X_2}{X_1}\right)} = \frac{\sqrt{\mu_o/\varepsilon_o}}{\frac{4}{\pi}\sqrt{\varepsilon_r}\ \ln\left(\frac{X_2}{X_1}\right)} \tag{2.15}$$

where

$$-\frac{\pi W}{4h} = \frac{1 - X_1^2}{2} + \ln(X_2)] \tag{2.16a}$$

and

$$-\frac{\pi W}{4h} = \frac{1 - X_2^2}{2} + \ln(X_2) \tag{2.16b}$$

$$0 < X_1 < 1 \qquad \text{and} \qquad X_2 > 1$$

It is worth noting that when $\frac{W}{h} > 1$, $X_1 << 1$ and $X_2 >> 1$, and equations (2.16a) and (2.16b) can be approximated by:

$$-\frac{W}{4h} \cong \frac{1}{2} + \ln(X_1)$$

or

$$\ln(X_1) \cong -\frac{1}{2}\left(1 + \frac{W}{2h}\right)$$

and

$$-\frac{W}{4h} \cong \frac{1 - X_2^2}{Z}$$

or

$$\ln(X_2) = \frac{1}{2}\ \ln\left(1 + \frac{W}{2h}\right)$$

$$\therefore \quad Z_o = \frac{\sqrt{\mu_o/\varepsilon_o}}{\frac{4}{\pi}\sqrt{\varepsilon_r}\left[\frac{1}{2}\ln\left(1 + \frac{\pi W}{2h}\right) + \frac{1}{2}\left(1 + \frac{\pi W}{2h}\right)\right]}$$

or

$$Z_o = \frac{\sqrt{\mu_o/\varepsilon_o}}{\sqrt{\varepsilon_r}\ \frac{W}{h}\ [\ 1 + \frac{2h}{\pi W}\ (1 + \ln\ (1 + \frac{\pi W}{2h}\ )\ ]} \tag{2.17}$$

Equation (2.17) is identical to the expression developed by Assadourian and Rimai[2] for the characteristic impedance of microstrip lines which they obtained using a different conformal mapping function, and gives good results for values of $W/h > 2$.

2.2 ANALYSIS OF MICROSTRIPLINES ON SINGLE LAYER DIELECTRIC SUBSTRATES USING THE VARIATIONAL METHOD:

(a) Negligible Strip Conductor Thickness

Consider the microstrip transmission line depicted in Figure 2.6. The static potential distribution $\phi(x,y)$ in the line structure must satisfy Poisson's equation:

$$\nabla^2\ \phi(x,y) = -\frac{\rho(x,y)}{\varepsilon_o\,\varepsilon_r} \tag{2.18}$$

where $\rho(x,y)$ = charge distribution on the surface of the conducting strip.

ε_r = relative dielectric constant of the substrate.

ε_o = permittivity of free space = $\frac{1}{36\pi} \times 10^{-9}$ far./m.

The line capacitance of the microstrip line can be obtained from the variational expression[22]:

$$\frac{1}{C} = \frac{\int_s \rho(x,y)\ \phi(x,y)d\ell}{\left[\int_s \rho(x,y)d\ell\right]^2} \tag{2.19}$$

where the integration is carried out around the conducting strip.

Assuming that the microstrip line will propagate a pure TEM mode, the characteristic impedance and guide wavelength of the structure will be given by:

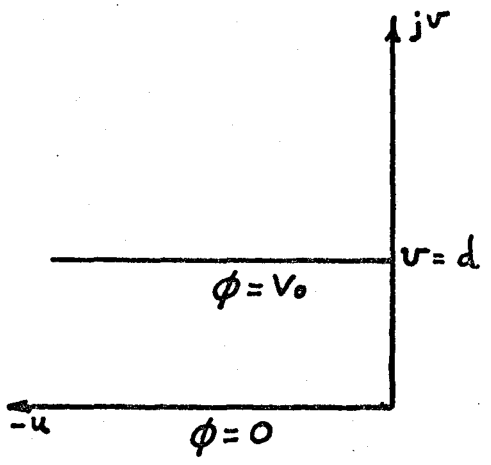

FIGURE 2.1: A Semi-infinite parallel-plate capacitor

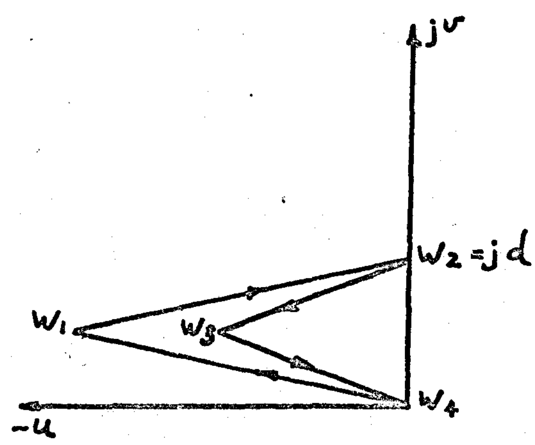

FIGURE 2.2: To obtain capacitor boundaries in W plane

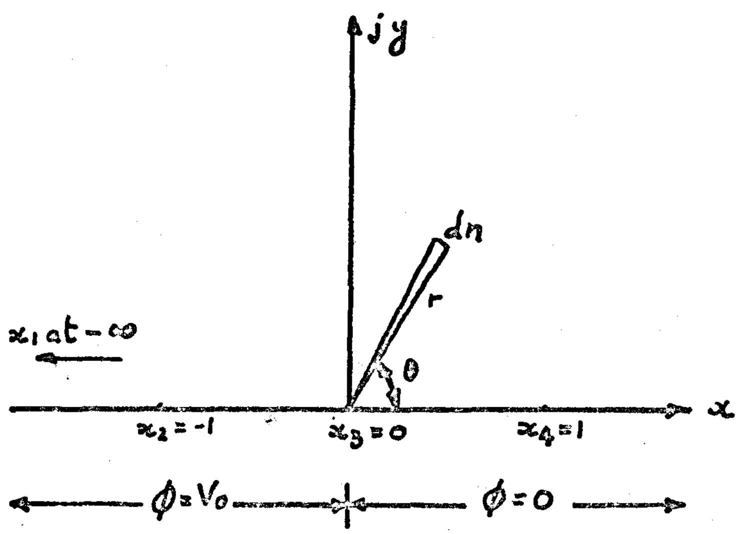

FIGURE 2.3: Capacitor boundaries in the Z plane

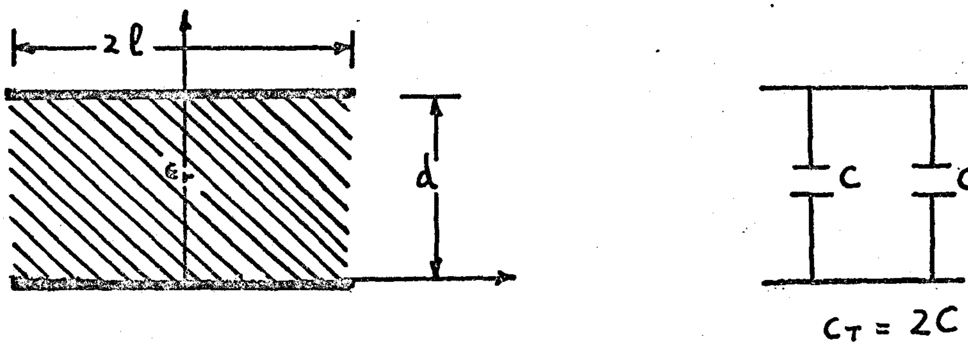

FIGURE 2.4: A parallel-plate capacitor of width 2ℓ and plate separation d

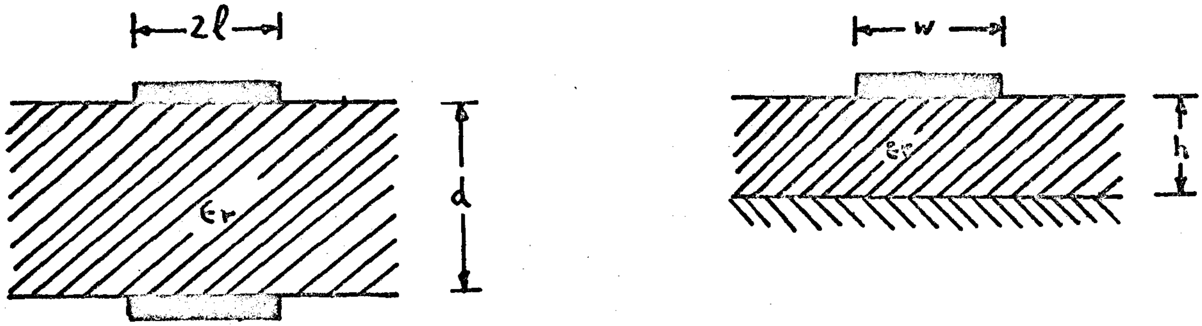

FIGURE 2.5: Comparison between parallel-plane and microstrip structures

$$Z_o = \frac{1}{v_o\sqrt{CC_o}} = \sqrt{\frac{C_o}{C}}\; Z'_o \tag{2.20a}$$

and

$$\lambda = \sqrt{\frac{C_o}{C}}\; \lambda_o \tag{2.20b}$$

where

v_o = velocity of light in free space $\cong 2.998 \times 10^8$ m/sec

C_o = line capacitance without dielectric

C = line capacitance with dielectric present

Z'_o = characteristic impedance of the line in free space

λ_o = free space wavelength

Since the strip conductor is infinitely thin, the charge distribution will be given by:

$$\rho(x,y) = f(x)\ \delta(y-h) \tag{2.21}$$

where

$\delta(y-h)$ = Dirac's delta function

= ∞ when $y = h$

= 0 otherwise

Since the line structure is symmetric about the y-axis, f(x) is an even function of x.

The Fourier transform $F(\beta)$ of $f(x)$ is defined by:

$$F(\beta) = \int_{-\infty}^{\infty} f(x)\ e^{j\beta x}\ dx \tag{2.22a}$$

Conversely

$$f(x) = \frac{1}{2\pi} \int_{-\infty}^{\infty} F(\beta) e^{-j\beta x}\ d\beta \tag{2.2b}$$

Similarly, the Fourier transform $\Phi(\beta,y)$ of $\phi(x,y)$ will be given by:

$$\Phi(\beta,y) = \int_{-\infty}^{\infty} \phi(x,y)e^{j\beta x}\, dx \tag{2.23a}$$

and

$$\phi(x,y) = \frac{1}{2\pi} \int_{-\infty}^{\infty} \Phi(\beta,y)e^{-j\beta x}\, d\beta \tag{2.23b}$$

Using the above definitions in equation (2.18) gives:

$$\left(\frac{d^2}{dx^2} + \frac{d^2}{dy^2}\right) \frac{1}{2\pi} \int_{-\infty}^{\infty} \Phi(\beta,y)e^{-j\beta x}\, d\beta = 0 \qquad y \neq h$$

$$\therefore \quad \left(-\beta^2 + \frac{d^2}{dy^2}\right) \frac{1}{2\pi} \int_{-\infty}^{\infty} \Phi(\beta,y)e^{-j\beta x} d\beta = 0$$

or

$$\left(-\beta^2 + \frac{d^2}{dy^2}\right) \Phi(\beta,y) = 0 \qquad y \neq h \tag{2.24}$$

The boundary and continuity conditions in the Fourier domain are given by:

$$\Phi(\beta,0) = 0 \tag{2.25a}$$

$$\Phi(\beta,\infty) = 0 \tag{2.25b}$$

$$\Phi(\beta,h+0) = \Phi(\beta,h-0) \tag{2.25c}$$

$$\frac{d}{dy}\Phi(\beta,h+0) = \varepsilon_r \frac{d}{dy}\Phi(\beta,h-0) - \frac{F(\beta)}{\varepsilon_o} \tag{2.25d}$$

The solutions of equations(2.24) are:

$$\Phi(\beta,y) = A\, e^{\beta y} + Be^{-\beta y} \qquad 0 \leqslant y \leqslant h \tag{2.26a}$$

and

$$\Phi(\beta,y) = C\, e^{\beta y} + D\, e^{-\beta y} \qquad y \geqslant h \tag{2.26b}$$

Where A, B, C, and D are arbitrary constants which can be determined from the boundary conditions of the structure.

Since $(\Phi, 0) = 0$

$$\therefore \quad A + B = 0$$

or $$A = -B \tag{2.27a}$$

Similarly, since $\Phi(\beta, \infty) = 0$

$$\therefore \quad C = 0 \tag{2.27b}$$

Substituting equations (2.27a) and (2.27b) in equations (2.26a) and (2.26b) gives:

$$\Phi(\beta, y) = A[e^{\beta y} - e^{-\beta y}] \qquad 0 \leq y \leq h$$

and

$$\Phi(\beta, y) = D\, e^{-\beta y} \qquad y \geq h$$

<u>At y = h</u>

$$\Phi(\beta, h) = A[e^{\beta h} - e^{-\beta h}] = D\, e^{-\beta h}$$

$$\therefore \quad \frac{D}{A} = e^{2\beta h} - 1 \tag{2.28}$$

Equation (2.25d) can be written as:

$$-D\beta e^{-\beta h} = \varepsilon_r[\beta A(e^{\beta h} + e^{-\beta h})] - \frac{F(\beta)}{\varepsilon_o} \tag{2.29}$$

By substituting equation (2.28) in equation (2.29) one gets:

$$A = \frac{F(\beta)}{\varepsilon_o \beta[(e^{\beta h} - e^{-\beta h}) + \varepsilon_r(e^{\beta h} + e^{-\beta h})]} \tag{2.30}$$

And since
$$\Phi(\beta, h) = A(e^{\beta h} - e^{-\beta h})$$

$$\therefore \quad \Phi(\beta, h) = \frac{F(\beta)\ (e^{\beta h} - e^{-\beta h})}{\varepsilon_o \beta[(e^{\beta h} - e^{-\beta h}) + \varepsilon_r(e^{\beta h} + e^{-\beta h})]}$$

or

$$\Phi(\beta,h) = \frac{F(\beta)}{\varepsilon_o \beta[1 + \varepsilon_r \coth(\beta h)]} \tag{2.31}$$

From equation (2.19), the line capacitance of a microstrip line of strip width W can be written as:

$$\frac{1}{C} = \frac{\int_{-W/2}^{W/2} f(x)\ \phi(x,h)dx}{\left[\int_{-W/2}^{W/2} f(x)dx\right]^2} \tag{2.32}$$

By using Parseval's theorem, the line capacitance will be given by:

$$\frac{1}{C} = \frac{1}{2\pi} \frac{\int_{-\infty}^{\infty} F(\beta)\ \Phi(\beta,h)d\beta}{\left[\int_{-W/2}^{W/2} f(x)dx\right]^2} \tag{2.33}$$

Substituting equation (2.31) in equation (2.33) gives:

$$\frac{1}{C} = \frac{1}{\pi\varepsilon_o} \frac{\int_{o}^{\infty} \frac{[F(\beta)]^2\ d(\beta h)}{[1 + \varepsilon_r \coth(\beta h)]\beta h}}{\left[\int_{-W/2}^{W/2} f(x)dx\right]^2} \tag{2.34}$$

where $F(\beta) = \int_{-\infty}^{\infty} f(x)e^{j\beta x}\ dx$

In order to be able to compute the line capacitance of the microstrip line, the charge distribution f(x) must be known. Since this is a variational method, the function f(x) which maximizes the capacitance will give the closest value to the exact result for the line capacitance. Therefore the following functions will be investigated:

(i) $$f(x) = \begin{cases} \text{constant } k & -\frac{W}{2} \leq x \leq \frac{W}{2} \\ 0 & \text{Otherwise} \end{cases}$$

$$\therefore \quad \frac{\int_{-\infty}^{\infty} f(x) e^{j\beta x}\, dx}{\int_{-W/2}^{W/2} f(x)\, dx} = \frac{\int_{-W/2}^{W/2} k\, e^{j\beta x}\, dx}{\int_{-W/2}^{W/2} k\, dx} = \frac{\sin\left(\frac{\beta W}{2}\right)}{\left(\frac{\beta W}{2}\right)}$$

$\therefore$ for $f(x) = k$,

$$\frac{1}{C} = \frac{1}{\pi\varepsilon_o} \int_o^{\infty} \left[\frac{\sin\left(\frac{\beta W}{2}\right)}{\left(\frac{\beta W}{2}\right)}\right]^2 \frac{1}{[1 + \varepsilon_r \coth(\beta h)]}\, d\beta h \tag{2.35}$$

(ii) $$f(x) = \begin{cases} |x| & -\frac{W}{2} \leq x \leq \frac{W}{2} \\ 0 & \text{otherwise} \end{cases}$$

$$\frac{F(\beta)}{\left[\int_{-W/2}^{W/2} f(x)\, dx\right]} = \frac{\int_o^{W/2} |x|\, e^{j\beta x}\, dx + \int_{-W/2}^{0} |x|\, e^{j\beta x}\, dx}{\int_{-W/2}^{W/2} |x|\, dx}$$

Substituting $x = -x$ in the second integral in the numerator gives:

$$\frac{F(\beta)}{\int_{-W/2}^{W/2} f(x)dx} = \frac{\int_o^{W/2} 2|x| \cos(\beta x)dx}{(W/2)^2}$$

$$= \frac{2}{(W/2)^2} \left[\frac{W}{2\beta} \sin\left(\frac{\beta W}{2}\right) + \frac{1}{\beta^2} \cos\left(\frac{\beta W}{2}\right) - \frac{1}{\beta^2} \right]$$

$$= \frac{2 \sin\left(\frac{\beta W}{2}\right)}{\frac{\beta W}{2}} - \left[\frac{\sin\left(\frac{\beta W}{4}\right)}{\frac{\beta W}{4}}\right]^2$$

$$\therefore \quad \frac{1}{C} = \frac{1}{\varepsilon_o} \int_o^\infty \left\{ \frac{\left(\dfrac{2\sin(\frac{\beta W}{2})}{\frac{\beta W}{2}} - \left[\dfrac{\sin(\frac{\beta W}{2})}{\frac{\beta W}{4}} \right]^2 \right)^2}{[1 + \varepsilon_r \coth(\beta h)]\beta h} \right\} d\beta h \qquad (2.36)$$

$$\text{(iii)} \quad f(x) = \begin{cases} x^2 & -\frac{W}{2} \leqslant x \leqslant \frac{W}{2} \\ 0 & \text{otherwise} \end{cases}$$

$$\frac{F(\beta)}{\int_{-W/2}^{W/2} f(x)dx} = \frac{\int_o^{W/2} 2x^2 \cos(\beta x)dx}{\frac{2}{3}\left(\frac{W}{2}\right)^3}$$

$$= \frac{2}{W^3/12} \left[\frac{x^2}{\beta} \sin(\beta x) + \frac{2x}{\beta^2} \cos(\beta x) - \frac{2}{\beta^3} \sin \beta x \right]_0^{W/2}$$

$$= \frac{3\sin(\frac{\beta W}{2})}{\frac{\beta W}{2}} + \frac{6\cos(\frac{\beta W}{2})}{(\frac{\beta W}{2})^3} - \frac{6\sin(\frac{\beta W}{2})}{(\frac{\beta W}{2})^3}$$

$$\therefore \quad \frac{1}{C} = \frac{1}{\pi\varepsilon_o} \int_o^\infty \left\{ \frac{\left[\dfrac{3\sin(\beta W/2)}{(\beta W/2)} + \dfrac{6\cos(\beta W/2)}{(\beta W/2)^2} - \dfrac{6\sin(\beta W/2)}{(\beta W/2)^3} \right]^2}{[1 + \varepsilon_r \coth(\beta h)]\beta h} \right\} d\beta h \qquad (2.37)$$

The three expressions for the line capacitance given by equations (2.35), (2.36), and (2.37) were integrated on an IBM 7040 digital computer using Simpson's Rule. It was found that maximum capacitance was obtained for the charge distribution function $f(x) = |x|$.

$$\frac{1}{C} = \frac{1}{\pi\varepsilon_o} \int_o^\infty \left\{ \frac{\left(\dfrac{2\sin(\beta W/2)}{(\beta W/2)} - \left[\dfrac{\sin(\beta W/4)}{(\beta W/4)} \right]^2 \right)^2}{[1 + \varepsilon_r \coth(\beta h)]\beta h} \right\} d\beta h \qquad (2.36)$$

In order to integrate equation (2.36), the limit of $\frac{1}{C}$ as $\beta h \to 0$ must be determined.

$$\lim_{\beta h \to 0} \frac{1}{C} = \lim_{\beta h \to 0} \frac{1}{\pi \varepsilon_o} \frac{\left\{ \frac{2 \sin(\beta h/2 \; W/h)}{\beta h/2 \quad W/h} - \left| \frac{\sin(\beta h/4 \quad W/h)}{\beta h/4 \quad W/h} \right|^2 \right\}^2}{\left[1 + \varepsilon_r \left(\frac{1 + 2\,\beta h + \ldots + 1)}{1 + 2\,\beta h + \ldots - 1} \right) \right] \beta h}$$

$$= \frac{1}{\pi \varepsilon_o} \frac{[2 - 1^2]^2}{\varepsilon_r}$$

$$\lim_{\beta h \to 0} \frac{1}{C} = \frac{1}{\pi \varepsilon_o \varepsilon_r} \tag{2.37}$$

(b) Finite Strip Conductor Thickness

When the strip conductor has a finite thickness t compared to the substrate thickness (see Figure 2.7), the formulas developed in (a) will have to be modified.

It is evident that the potential function $\Phi(\beta,y)$ in the region above $y = h$ will have an exponential behaviour $e^{-\beta y}$.

$$\Phi(\beta, h + t) = e^{-\beta t} \, \Phi(\beta, h) \tag{2.38}$$

where t = conductor thickness.

By considering two layers of charge at $y = h$ and $y = h+t$, the boundary and continuity conditions in the Fourier domain become:

$$\Phi(\beta, 0) = 0 \tag{2.39a}$$

$$\Phi(\beta, \infty) = 0 \tag{2.39b}$$

$$\Phi(\beta, h+0) = \Phi(\beta, h-0) \tag{2.39c}$$

$$\frac{d}{dy}\Phi(\beta,h+0) = \varepsilon_r \frac{d}{dy}\Phi(\beta,h-0) - \frac{F(\beta)}{\varepsilon_o} \tag{2.39d}$$

$$\Phi(\beta,\ h+t+0) = \Phi(\beta,\ h+t-0) \tag{2.39e}$$

$$\frac{d}{dy}\Phi(\beta,\ h+t+0) = \frac{d}{dy}\Phi(\beta,\ h+t-0) - \frac{F(\beta)}{\varepsilon_o} \tag{2.39f}$$

Using the above boundary conditions in equations (2.26a) and 2.26b) gives the modified expression for the line capacitance:

$$\frac{1}{C} = \frac{1}{\pi\varepsilon_o} \frac{\left\{ \int_o^\infty \left(\frac{1+e^{-\beta t}}{2}\right) \frac{[F(\beta)]^2 \ d(\beta h)}{[1+\varepsilon_r \coth(\beta h)]\beta h} \right\}}{\left[\int_s f(x)dx \right]^2} \tag{2.40}$$

2.3 MICROSTRIP LINES ON TWO-LAYER DIELECTRIC SUBSTRATES:

(a) Negligible Conductor Thickness

Let the relative dielectric constants of the two dielectrics be given by ε_1 and ε_2 respectively as depicted in Figure 2.8.

The D.E. which defines the static potential distribution in the Fourier domain is given by equation (2.24), i.e. -

$$\left[-\beta^2 + \frac{d^2}{dy^2} \right] \Phi(\beta,\ y) = 0 \qquad y \neq b,h$$

The boundary and continuity conditions of the structure will become:

$$\Phi(\beta,\ 0) = 0 \tag{2.41a}$$

$$\Phi(\beta,\ \infty) = 0 \tag{2.41b}$$

$$\Phi(\beta,\ h+0) = \Phi(\beta,\ h-0) \tag{2.41c}$$

$$\varepsilon_2 \frac{d}{dy}\Phi(\beta,\ h+0) = \varepsilon_1 \frac{d}{dy}\Phi(\beta,\ h-0) \tag{2.41d}$$

$$\Phi(\beta,\ b+0) = \Phi(\beta,\ b-0) \tag{2.41e}$$

$$\frac{d}{dy}\Phi(\beta,\ b+0) = \varepsilon_2 \frac{d}{dy}\Phi(\beta,\ b-0) - \frac{F(\beta)}{\varepsilon_o} \tag{2.41f}$$

The solutions of the D.E in the two dielectrics as well as the free space above them are:

$$\Phi(\beta, y) = A e^{\beta y} + B e^{-\beta y} \qquad 0 \leq y \leq h \qquad (2.42a)$$

$$\Phi(\beta, y) = C e^{\beta y} + D e^{-\beta y} \qquad h \leq y \leq b \qquad (2.42b)$$

and $$\Phi(\beta, y) = E e^{\beta y} + F e^{-\beta y} \qquad y \geq b \qquad (2.42c)$$

where A, B, C, D, E, and F are arbitrary constants to be determined from the boundary conditions.

Since $\Phi(\beta, 0) = 0$

$\therefore \quad A = -B$

and $$\Phi(\beta, y) = A(e^{\beta y} - e^{-\beta y}) \qquad 0 \leq y \leq h \qquad (2.43a)$$

Similarly, since $\Phi(\beta, \infty) = 0$ $\quad \therefore \ E = 0$

and $$\Phi(\beta, y) = F e^{-\beta y} \qquad y \geq b \qquad (2.43b)$$

<u>At $y = h$</u>

$$\Phi(\beta, h) = A(e^{\beta h} - e^{-\beta h}) = C e^{\beta h} + D e^{-\beta h} \qquad (2.43c)$$

And equation (2.41d) becomes:

$$\varepsilon_2[C e^{\beta h} - D e^{-\beta h}] = \varepsilon_1 A[e^{\beta h} + e^{-\beta h}] \qquad (2.43d)$$

<u>At $y = b$</u>

$$\Phi(\beta, b) = C e^{\beta b} + D e^{-\beta b} = F e^{-\beta b}$$

Substituting in equation (2.41f)

$$-F \beta e^{-\beta b} = \beta\varepsilon_2[C e^{\beta b} - D e^{-\beta b}] - \frac{F(\beta)}{\varepsilon_o}$$

or

$$-(C e^{+\beta b} + D e^{-\beta b}) = \varepsilon_2(C e^{\beta b} - D e^{-\beta b}) - \frac{F(\beta)}{\varepsilon_o \beta}$$

Giving by rearranging,

$$C(\varepsilon_2+1)e^{\beta b} + D(1-\varepsilon_2)e^{-\beta b} - \frac{F(\beta)}{\varepsilon_o\beta} = 0 \tag{2.43e}$$

Dividing equation (2.43c) by equation (2.43d) gives:

$$\frac{C\ e^{\beta h} + D\ e^{-\beta h}}{C\ e^{\beta h} - D\ e^{-\beta h}} = \frac{\varepsilon_2(e^{\beta h} - e^{-\beta h})}{\varepsilon_1(e^{\beta h} + e^{-\beta h})}$$

from which,

$$\frac{C}{D} = \frac{(\varepsilon_2 + \varepsilon_1) - (\varepsilon_2 - \varepsilon_1)e^{-2\beta h}}{(\varepsilon_2 - \varepsilon_1)e^{2\beta h} - (\varepsilon_2 + \varepsilon_1)} \tag{2.44}$$

Substituting $\frac{C}{D}$ in equation (2.43e),

$$C = \frac{F(\beta)}{\varepsilon_o\beta[\varepsilon_2+1)e^{\beta b} - \left\{\dfrac{(\varepsilon_2-\varepsilon_1)e^{2\beta h} - (\varepsilon_2+\varepsilon_1)}{(\varepsilon_2+\varepsilon_1) - (\varepsilon_2-\varepsilon_1)e^{-2\beta h}}\right\}(\varepsilon_2 - 1)e^{-\beta b}]}$$

and

$$D = \frac{F(\beta)}{\varepsilon_o\beta\left[\left\{\dfrac{(\varepsilon_2+\varepsilon_1) - (\varepsilon_2-\varepsilon_1)e^{-2\beta h}}{(\varepsilon_2-\varepsilon_1)e^{2\beta h} - (\varepsilon_2+\varepsilon_1)}\right\}(\varepsilon_2 + 1)e^{\beta b} - (\varepsilon_2 - 1)e^{-\beta b}\right]}$$

Let

$$\left.\begin{aligned} r &= \varepsilon_2 - \varepsilon_1 \\ s &= \varepsilon_2 + \varepsilon_1 \\ t &= \varepsilon_2 - 1 \\ p &= \varepsilon_2 + 1 \end{aligned}\right\} \tag{2.45}$$

Then C and D can be written as:

$$C = \frac{F(\beta)}{\varepsilon_o\beta[pe^{\beta b} - \left\{\dfrac{(re^{2\beta h} - s)te^{-\beta b}}{s - re^{-2\beta h}}\right\}]} \tag{2.46a}$$

and

$$D = \frac{F(\beta)}{\varepsilon_o\beta[\left\{\dfrac{s - re^{-2\beta h}}{re^{2\beta h} - s}\right\} pe^{\beta b} - te^{-\beta b}]} \tag{2.46b}$$

Substititing for C and D in equation (2.42b) (at y = b) gives:

$$\Phi(\beta, b) = \frac{F(\beta)}{\varepsilon_0\beta}\left[\frac{1}{p - \left\{\dfrac{(re^{2\beta h} - s)}{s - re^{-2\beta h}} te^{-2\beta b}\right\}} + \frac{1}{\left\{\left(\dfrac{s - re^{-2\beta h}}{re^{2\beta h} - s}\right) pe^{2\beta b} - t\right\}}\right] \tag{2.47}$$

<u>Special Case</u>: If $\varepsilon_1 = \varepsilon_2 = \varepsilon_r$ and $b/h = 1$, it follows that $r = 0$, $S = 2\varepsilon_r$, $t = \varepsilon_r - 1$, and $p = \varepsilon_r + 1$.

$$\therefore \Phi(\beta, h) = \frac{F(\beta)}{\varepsilon_o\beta}\left[\frac{1}{(\varepsilon_r + 1) + \left\{\dfrac{(0 - 2\varepsilon_r)}{2\varepsilon - 0} (\varepsilon_r - 1)e^{-2\beta h}\right\}} + \frac{1}{\left\{\dfrac{2\varepsilon_r}{-2\varepsilon_r} (\varepsilon_r + 1)e^{+2\beta h} - (\varepsilon_r - 1)\right\}}\right]$$

$$= \frac{F(\beta)}{\varepsilon_o\beta} \frac{\left[e^{2\beta h} - 1\right]}{(\varepsilon_r + 1)e^{2\beta h} + (\varepsilon_r - 1)e^{-2\beta h}}$$

or $$\Phi(\beta, h) = \frac{F(\beta)}{\varepsilon_o \beta} \left[\frac{1}{1 + \varepsilon_r \coth(\beta h)} \right]$$

which is identical to equation (2.31) developed in section (2.2).

Therefore the line capacitance of a microstrip line on a two-layer dielectric substrate will be given by:

$$\frac{1}{C} = \frac{\frac{1}{\pi\varepsilon_o} \int_o^\infty \left\{ \frac{[F(\beta)]^2}{\beta h} \left[\frac{1}{p - \left(\frac{re^{2\beta h} - s}{s - re^{-2\beta h}}\right) te^{-2\beta b}} + \frac{1}{\left(\frac{s - re^{-2\beta h}}{re^{2\beta h} - s}\right) pe^{2\beta b} - t} \right] \right\} d\beta h}{\left[\int_{-W/2}^{W/2} f(x)\,dx \right]^2} \quad \text{----------- (2.48)}$$

Since the charge distribution function $f(x) = |x|$ gives the maximum value for the line capacitance, it follows that

$$\frac{1}{C} = \frac{1}{\pi\varepsilon_o} \int_o^\infty \frac{1}{\beta h} \left[\left\{ \frac{2 \sin\left(\frac{\beta h}{2} \cdot \frac{W}{h}\right)}{\frac{\beta h}{2} \cdot \frac{W}{h}} - \left[\frac{\sin\left(\frac{\beta h}{4} \cdot \frac{W}{h}\right)}{\frac{\beta h}{4} \cdot \frac{W}{h}} \right]^2 \right\}^2 \times \right.$$
$$\left. \left\{ \frac{1}{\left[p - \left(\frac{re^{2\beta h} - s}{s - re^{-2\beta h}}\right) te^{-2\beta h . Y}\right]} + \frac{1}{\left[\left(\frac{s - re^{-2\beta h}}{re^{2\beta h} - s}\right) pe^{2\beta h . Y} - t\right]} \right\} \right] d(\beta h) \quad \text{----------- (2.49)}$$

where $Y = b/h$.

To integrate equation (2.49) numerically the limit of $\frac{1}{C}$ as $\beta h \to 0$ must be known.

$$\text{If} \quad A = \left\{ \frac{2\sin\left(\frac{\beta h}{2} \cdot \frac{W}{h}\right)}{\frac{\beta h}{2} \cdot \frac{W}{h}} - \left[\frac{\sin\left(\frac{\beta h}{4} \cdot \frac{W}{h}\right)}{\frac{\beta h}{4} \cdot \frac{W}{h}} \right]^2 \right\}^2$$

and

$$B = \frac{1}{\beta h} \left[\frac{1}{[p - \left(\frac{re^{2\beta h} - s}{s - re^{-2\beta h}}\right) te^{-2\beta hY}]} + \frac{1}{[\left(\frac{s - re^{-s\beta h}}{re^{2\beta h} - s}\right) pe^{2\beta hY} - t]} \right]$$

Then $\lim\limits_{\beta h \to 0} A = \{2 \times 1 - 1^2\}^2 = 1$

and $\lim\limits_{\beta h \to 0} B = \frac{1}{0} \left[\frac{1}{p+t} - \frac{1}{p+t} \right]$

which is indeterminate.

Differentiating the numerator and denominator of B gives:

$$\lim_{\beta h \to 0} B = \lim_{\beta h \to 0} \left[\left\{ \frac{[s-re^{2\beta h})p.2Y\ e^{2\beta hY} + 2re^{-2\beta h}pe^{2\beta hY}](re^{2\beta h}-s)-(s-re^{-2\beta h})pe^{2\beta hY}2re^{2\beta h}}{(re^{2\beta h} - s)^2} \right\} \right.$$

$$- \left\{ \frac{[(re^{2\beta h}-s).-2Yte^{-2\beta hY} + 2re^{2\beta h}te^{-2\beta hY}](s-re^{-2\beta h})-(re^{2\beta h}-s)te^{-2\beta hY}2re^{2\beta h}}{(s - re^{-2\beta h})^2} \right\}$$

$$\left. \div \left\{ [p - \left(\frac{re^{2\beta h}-s}{s-re^{-2\beta h}}\right) te^{-2\beta h.Y}][\left(\frac{s-re^{-2\beta h}}{re^{2\beta h}-s}\right) pe^{-2Y\beta h} - t] + 0 \right\} \right]$$

From which

$$\lim_{\beta h \to 0} B = \left[\left\{ \frac{[(s - r)2pY + 2rp]\ (r - s) - (s - r)2rp}{(r - s)^2} \right\} \right.$$

(Equation continued) ----

$$- \left\{ \frac{[(r - s).-2Yt + 2rt]\ (s - r) - (r - s)2rt}{(s - r)^2} \right\}$$

$$\left. \div\ [-\ (p + t)^2] \right]$$

$$= \frac{2Y}{p+t} + \frac{4r}{(p+t)(s-r)} \tag{2.50}$$

$$\text{and} \quad \lim_{\beta h \to 0} \frac{1}{C} = \frac{1}{\pi \varepsilon_o} \left[\frac{2Y}{(p+t)} + \frac{4r}{(p+t)(s-r)} \right] \tag{2.51}$$

Special case: If $\varepsilon_1 = \varepsilon_2 = \varepsilon_r$ and $Y = 1$

$$\therefore \lim_{\beta h \to 0} \frac{1}{C} = \frac{1}{\pi \varepsilon_o} \left[\frac{2 \times 1}{2\varepsilon_r} + 4 \times 0 \right]$$

$$= \frac{1}{\pi \varepsilon_o \varepsilon_r}$$

Which is identical to equation (2.37) developed in section (2.2).

(b) Finite Strip Conductor Thickness

For a finite strip conductor thickness, a similar analysis as that described in (b) of section (2.1) can be applied. The boundary and continuity conditions in the Fourier domain of such a structure (see Figure 2.8) become:

$$\Phi(\beta, o) = 0 \tag{2.52a}$$

$$\Phi(\beta, \infty) = 0 \tag{2.52b}$$

$$\Phi(\beta, h+0) = \Phi(\beta, h-0) \tag{2.52c}$$

$$\varepsilon_2 \frac{d}{dy} \Phi(\beta, h+0) = \varepsilon_1 \frac{d}{dy} \Phi(\beta, h-0) \tag{2.52d}$$

$$\Phi(\beta,\ b+0) = \phi(\beta,\ b-0) \tag{2.52e}$$

$$\frac{d}{dy}\ \phi(\beta,\ b+0) = \varepsilon_2 \frac{d}{dy}\ \Phi(\beta,\ b-0) - \frac{F(\beta)}{\varepsilon_o} \tag{2.52f}$$

$$\Phi(\beta,\ b+t+0) = \Phi(\beta,\ b+t-0) \tag{2.52g}$$

$$\frac{d}{dy}\ \Phi(\beta,\ b+t+0) = \frac{d}{dy}\ \Phi(\beta,\ b+t-0) - \frac{F(\beta)}{\varepsilon_o} \tag{2.52h}$$

Noting that $\Phi(\beta,\ b+t) = e^{-\beta t}\ \Phi(\beta,\ b)$ one can obtain the modified expression for the line capacitance as:

$$\frac{1}{C} = \frac{1}{\pi\varepsilon_o} \int_o^\infty \left\{ \left(\frac{1+e^{-\beta t}}{2} \right) \frac{1}{\beta h} \left[\frac{2\ \sin\left(\frac{\beta h}{2} \cdot \frac{W}{h} \right)}{\frac{\beta h}{2} \cdot \frac{W}{h}} - \left[\frac{\sin\left(\frac{\beta h}{4} \cdot \frac{W}{h} \right)}{\frac{\beta h}{4} \cdot \frac{W}{h}} \right]^2 \right]^2 \text{X} \right.$$
$$\left. \left[\frac{1}{\left\{ p - \left(\frac{re^{2\beta h}-s}{s-re^{-\beta h}} \right) te^{-2\beta h} \right\}} + \frac{1}{\left\{ \left(\frac{s-re^{-2\beta h}}{re^{2\beta h}-s} \right) pe^{2\beta b} - t \right\}} \right] d(\beta h) \right. \tag{2.53}$$

2.3 ATTENUATION OF MICROSTRIP LINES ON SEMICONDUCTOR SUBSTRATES

The loss per unit length of a microstrip transmission line on a semiconductor substrate is given by:

$$\alpha = \alpha_c + \alpha_g + \alpha_s \tag{2.54}$$

where

α_c = Loss in the conductor in nepers/m.

α_g = Loss in the ground plane in nepers/m.

α_s = Loss in the semiconductor substrate in nepers/m.

In order to simplify the analysis it is assumed that the current distributions across the width of the strip conductor and in the ground plane under the conductor are uniform. In this case

$$\alpha_c + \alpha_g = \frac{r_1 + r_2}{2Z_o} \tag{2.55}$$

where r_1 and r_2 are the effective series resistance per unit length of the strip conductor and ground plane respectively, and Z_o is the characteristic impedance of the line.

If δ_1 and δ_2 = skin depths of the conductor and ground plane respectively,

σ_1 and σ_2 = conductivity of the conductor and ground plane respectively,

then $r_1 + r_2 = \dfrac{1}{\sigma_1 \delta_1 W} + \dfrac{1}{\sigma_2 \delta_2 W}$

where W = width of strip conductor.

Substituting in equation (2.55),

$$\alpha_c + \alpha_g = \frac{\sqrt{\pi f \mu}}{2\ Z_o W} \left(\frac{1}{\sqrt{\sigma_1}} + \frac{1}{\sqrt{\sigma_2}} \right) \tag{2.56}$$

The semiconductor (dielectric) loss will be given by:

$$\alpha_s = \frac{g\ Z_o}{2} \tag{2.57}$$

where g = effective conductance representing total dielectric losses in mho/m

$= \dfrac{1}{\rho_s} \dfrac{W}{h}$.

Where ρ_s = resistivity of the semiconductor substrate in ohm-m.

$$\therefore \quad \alpha_s = \frac{Z_o}{2\rho_s} \frac{W}{h}$$

∴ total attenuation in the microstrip line will be given by:

$$\alpha = \frac{\sqrt{\pi f \mu}}{2 Z_o W} \left[\frac{1}{\sqrt{\sigma_1}} + \frac{1}{\sqrt{\sigma_2}} \right] + \frac{Z_o W}{2 \rho_s h} \text{ nepers/m} \qquad (2.58)$$

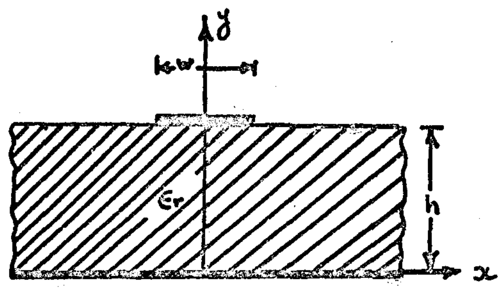

FIGURE 2.6: Microstrip Line with Negligible Strip Thickness

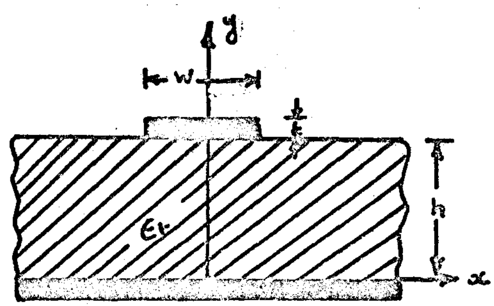

FIGURE 2.7: Microstrip Line with Finite Strip Thickness t < W

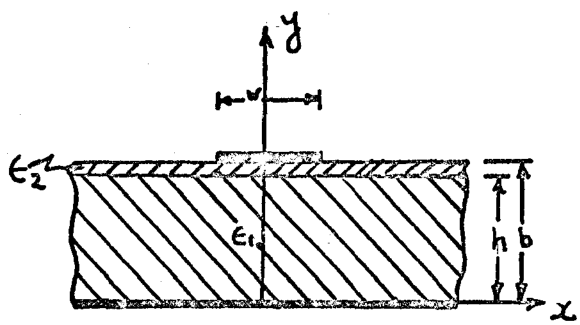

FIGURE 2.8: Microstrip Line on a Two Layer Dielectric with Negligible Strip Thickness

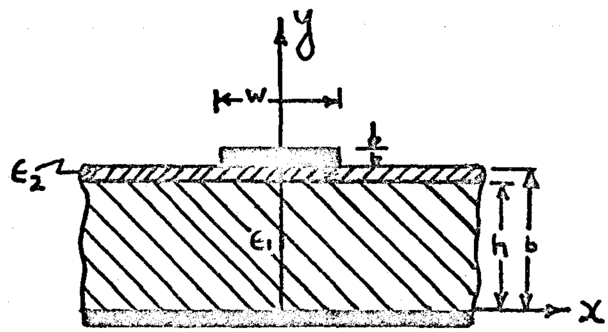

FIGURE 2.9: Microstrip Line on a Two Layer Dielectric with Negligible Strip Thickness

CHAPTER III

THEORY OF MEASUREMENT

3.1 INTRODUCTION:

The best description of a waveguide junction from the view point of power relations is the scattering matrix[23]. However, J.E. Storer, et al[24] have shown that the scattering matrix is also the best description for a junction between any two guiding systems.

The simplest method for the determination of the scattering matrix of a lossy two-port junction is that originally proposed by G. Deschamps in 1953[25] and which bears his name. M. Arditi[5] and T.M. Hyltin[15] applied this method in their experimental work on microstrip lines. M. Arditi used a sliding short on his line to obtain the scattering parameters of the lossy coaxial to microstrip transition, while T. M. Hyltin changed the microwave source frequency to obtain the same effect. However, to the author's knowledge all the experimental work on microstrip lines using the Deschamps' method has been carried using coaxial systems.

3.2 THE SCATTERING MATRIX:

Consider the two-port junction shown in Figure 3.1. The incident and reflected voltage waves at plane A are given in magnitude and phase by V_{A^+} and V_{A^-}, respectively, and at plane B by V_{B^+} and V_{B^-} respectively. The normalized incident and reflected waves will therefore be given by:

$$a_1 = \frac{V_{A^+}}{\sqrt{Z_1}} \;, \quad b_1 = \frac{V_{A^-}}{\sqrt{Z_1}} \;, \quad a_2 = \frac{V_{B^+}}{\sqrt{Z_2}} \;, \text{ and } b_2 = \frac{V_{B^-}}{\sqrt{Z_2}} \qquad \text{---------} \quad (3.1)$$

where Z_1 and Z_2 are the characteristic impedances of lines (1) and (2) respectively.

The scattering parameters, which relate the two reflected waves to the two incident waves are defined by: -

$$b_1 = S_{11} a_1 + S_{12} a_2 \tag{3.2a}$$

$$b_2 = S_{21} a_1 + S_{22} a_2 \tag{3.2b}$$

where S_{11} = reflection coefficient at terminal A when B is matched.

S_{22} = reflection coefficient at terminal B when A is matched.

S_{12} = transmission coefficient from A to B.

S_{21} = transmission coefficient from B to A.

Equations (3.2a) and (3.2b) can be expressed in matrix form as follows:

$$\begin{bmatrix} b_1 \\ b_2 \end{bmatrix} = \begin{bmatrix} S_{11} & S_{12} \\ S_{21} & S_{22} \end{bmatrix} \begin{bmatrix} a_1 \\ a_2 \end{bmatrix} \tag{3.3a}$$

or

$$[b] = [S] [a] \tag{3.3b}$$

where

$$[S] = \begin{bmatrix} S_{11} & S_{12} \\ S_{21} & S_{22} \end{bmatrix} \tag{3.3c}$$

$$S_{12} = S_{21} \quad \text{due to reciprocity.}$$

[S] is known as the scattering matrix of the junction, and it is interesting to note that the planes A and B may be choosen at any arbitrary points on the lines (1) and (2).

The insertion loss of the junction, which is a measure of efficiency is given by[25]:

$$S_{12} = -20 \log_{10} |S_{12}| \text{ db} \tag{3.4}$$

3.3 THE DESCHAMPS' METHOD:

The experimental set-up is shown in Figure 3.2.

Let

$\rho_1 = \frac{b_1}{a_1}$ be the reflection coefficient at the input terminals.

$\rho_2 = \frac{a_2}{b_2}$ be the reflection coefficient at the output terminals.

Dividing equation (3.2a) by a_1 gives: -

$$\frac{b_1}{a_1} = S_{11} + S_{12}\frac{a_2}{a_1} = \rho_1 \tag{3.5a}$$

Dividing equation (3.2b) by a_2 gives: -

$$\frac{b_2}{a_2} = S_{21}\frac{a_1}{a_2} + S_{22} = \frac{1}{\rho_2}$$

or

$$\frac{a_2}{a_1} = \frac{S_{21}}{\frac{1}{\rho_2} - S_{22}} \tag{3.5b}$$

Solving equations (3.5a) and (3.5b),

$$\rho_1 = S_{11} + \frac{S_{12}\,S_{21}}{\frac{1}{\rho_2} - S_{22}}$$

and since $S_{12} = S_{21}$ by reciprocity,

$$\rho_1 = S_{11} + \frac{S_{12}^2}{\frac{1}{\rho_2} - S_{22}} \tag{3.6}$$

Equation (3.6) is a bilinear equation relating the reflection coefficient ρ_1 at terminal A to the reflection coefficient ρ_2 at terminal B.

If a sliding short is moved on line (2), then the locus of ρ_2 will be a unit circle $|\rho_2| = 1$. It will be proved that ρ_1 also lies on a circle, from which by simple constructions the scattering parameters of the junction S_{11}, S_{12} and S_{22} can be determined in magnitude and phase.

Let $\alpha = S_{11}$, $\beta = S_{12}^{\;2}$ and $\gamma = S_{22}$

Equatinn (3.6) can therefore be rewritten as:

$$\rho_1 - \alpha = \frac{\beta \cdot \rho_2}{1 - \gamma\,\rho_2} \tag{3.6a}$$

or

$$\rho_2 = \frac{(\rho_1 - \alpha)}{\beta + \gamma(\rho_1 - \alpha)}$$

Since $|\rho_2| = 1$

$$\frac{|\rho_1 - \alpha|^2}{|\beta + \gamma(\rho_1 - \alpha)|^2} = 1 \tag{3.7}$$

Using the theory of complex numbers, equation (3.7) reduces to:

$$(\rho_1 - \alpha)(\rho_1 - \alpha)^* = \beta\beta^* + \gamma\gamma^*(\rho_1 - \alpha)(\rho_1 - \alpha)^* + \beta\gamma^*(\rho_1 - \alpha)^* + \beta^*\gamma(\rho_1 - \alpha)$$

where the asterik denotes the complex conjugate, or

$$(1 - \gamma\gamma^*)(\rho_1 - \alpha)(\rho_1 - \alpha)^* - \beta\gamma^*(\rho_1 - \alpha)^* - \beta^*\gamma(\rho_1 - \alpha) - \beta\beta^* = 0$$

----------- (3.8)

Equation (3.8) can be rewritten as:

$$(\rho_1 - \alpha)(\rho_1 - \alpha)^* - p(\rho_1 - \alpha)^* - q(\rho_1 - \alpha) - g = 0 \tag{3.8a}$$

where

$$\left.\begin{aligned} p &= \frac{\beta\gamma^*}{1 - \gamma\gamma^*} \\ q &= \frac{\beta^*\gamma}{1 - \gamma\gamma^*} = p^* \end{aligned}\right\} \tag{3.9}$$

and $$g = \frac{\beta\beta^*}{1 - \gamma\gamma^*} \quad \text{(real)} \tag{3.9}$$

Adding the real term pp^* to both sides of equation (3.8a) gives:

$$(\rho_1 - \alpha)(\rho_1 - \alpha)^* - p(\rho_1 - \alpha)^* - p^*(\rho_1 - \alpha) + pp^* = g + pp^*$$

or

$$|\rho_1 - \alpha - p|^2 = g + pp^* = r^2 \tag{3.10}$$

where r is a real and positive quantity.

Equation (3.10) is the equation of a circle with centre at $(\alpha + p)$ and radius $r = [g + pp^*]^{1/2}$.

In terms of the scattering parameters: -

C is located at a + p, i.e. $S_{11} + \dfrac{S_{12}{}^2 S_{22}{}^*}{1 - |S_{22}|^2}$

Radius of the circle $r = [g + pp^*]^{1/2}$

$$= \left[\frac{\beta\beta^*}{1 - \gamma\gamma^*} + \frac{\beta\beta^*\ \gamma\gamma^*}{(1 - \gamma\gamma^*)^2}\right]^{1/2}$$

or

$$r = \frac{\beta\beta^*}{1 - \gamma\gamma^*} = \frac{|S_{12}|^2}{1 - |S_{22}|^2}$$

$\therefore \rho_1$ lies on a circle with centre $S_{11} + \left(\dfrac{S_{12}{}^2\ S_{22}{}^*}{1 - |S_{22}|^2}\right)$

and radius $\dfrac{|S_{12}|^2}{1 - |S_{22}|^2}$

As depicted in Figure 3.3, the diameters of the circle $|\rho_2| = 1$ are transformed into circles orthogonal to ρ_1 and intersecting at the point I, the image of the centre 0 of the unit circle.

The point I, known as the iconocentre of ρ_1 is given by

$$\rho_1\Big]_I = \left[S_{11} + \frac{S_{12}^{\;2}}{1/\rho_2 - S_{22}}\right]_{\rho_2 = 0} = S_{11} \qquad (3.11a)$$

$\therefore$ the coordinates of the point I will give S_{11} in magnitude and phase.

Referring to Figures 3.2 and 3.3, the scattering parameters of the unknown lossy junction can be determined by moving a sliding short on lines (2) by $\lambda_g/8$ and measuring the corresponding reflection coefficients in magnitude and phase looking into plane A.

If the Points P_1', P_2', P_3', and P_4' represent the coordinates of the reflection coefficients of points P_1, P_2, P_3 and P_4 measured from plane A, then the intersection of the arcs P_1', P_3' and P_2' and P_4' will determine I, while the four points will define the circle ρ_1 centre C. The distance

$$CI = \left|S_{11} + \frac{S_{12}^{\;2}\, S_{22}^{\;*}}{1 - |S_{22}|^2} - S_{11}\right| = \frac{|S_{12}|^2 |S_{22}^{\;*}|}{1 - |S_{22}|^2} = r|S_{22}|$$

$$\therefore\ |S_{22}| = \frac{CI}{r} \qquad (3.11b)$$

$$\text{and}\quad |S_{12}|^2 = r[1 - |S_{22}|^2] \qquad (3.11c)$$

The following theorem will be made use of in the determination of $\arg S_{12}$ and $\arg S_{22}$.

<u>Theorem</u>: If any two circles C_1 and C_2 intersect orthogonally at the points A and B, and if O is any point on the arc AB of the Circle C_2 and BO intersects the circle C_1 at the point M, then the diameter passing through M is parallel to the tangent of the circle C_2 at the point O.

Proof: Referring to Figure 3.4, since the circles C_1 and C_2 are orthogonal, then the tangents of the two circles at the point B must pass through the centres of the circles.

$$\text{Since } \angle(NBM) = \pi/2$$

$$\text{then } (\phi + \delta) = \pi/2.$$

Since the radius $C_2 0$ is perpendicular to the tangent at 0, then $\omega + \delta = \pi/2$.

$$\therefore \quad \omega = \phi$$

$$\text{But} \quad \omega = \theta$$

$$\therefore \quad \theta = \phi$$

i.e. the tangent at point 0 is parallel to the diameter MN.

For simplicity, it is first assumed that the planes A and B are chosen such that both S_{11} and S_{22} are real and positive.

Therefore as seen from Figure 3.5, $OI = S_{11}$ lies on the x-axis with,

$$\arg(CI) = \arg\left[\frac{S_{12}^{2}\, S_{22}^{*}}{1 - |S_{22}|^2}\right]$$

$$= 2 \arg S_{12} \qquad \text{since } S_{22} \text{ is real.}$$

If P' is the image of the point P(+1), then it will be given by:

$$S_{11} + \frac{S_{12}^{2}}{1 - S_{22}}$$

$$\therefore \arg(IP') = \arg\left(S_{11} + \frac{S_{12}^{2}}{1 - S_{22}}\right)$$

$\therefore$ ICP$'$ is a straight line.

Subsequently, if S_{11} and S_{22} have phases arg S_{11} and arg S_{22}, respectively, then arg S_{22} will in effect rotate all the points of the unit circle ρ_2

through an angle arg S_{22}. Similarly arg S_{11} will rotate the circle ρ_1 about the point C through an angle arg S_{11}.

Referring to Figure 3.6, the image of the point P(+1) will be the point Q' when arg $S_{22} = 0$, and the point P' when neither arg S_{11} nor arg S_{22} is zero. The diameter OP, is hence transformed into an arc of a circle $S'P'$ orthogonal to the circle ρ_2.

Therefore it immediately follows that:

arg S_{22} = angle between the tangent of arc $S'P'$ at point I and IC.

Making use of the above theorem, this angle is equal to the angle between CP'' and IC. And since arg CI = 2 arg S_{12} - arg S_{22}

2 arg S_{12} = angle between OP and CP''.

Summary:

Referring to Figure 3.6,

$$\left.\begin{aligned}
S_{11} &= OI \\
\arg S_{11} &= \angle(OI, OP) \\
S_{12} &= \sqrt{r(1 - |S_{22}|^2)} \\
\arg S_{12} &= \frac{1}{2}\angle(OP, CP'') \\
S_{22} &= \frac{CI}{r} \\
\arg S_{22} &= \angle(IC, CP'')
\end{aligned}\right\} \qquad (3.12)$$

3.4 THEORY OF THE REFLECTION BRIDGE:

Microwave bridges are most suitable for the application of the Deschamp's method since they can accurately measure both the magnitude and phase of the reflection coefficient at microwave frequencies.

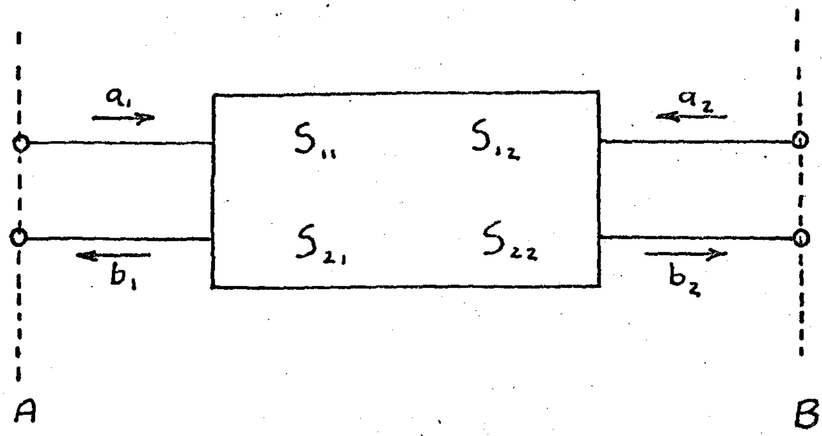

FIGURE 3.1: A Two-port Junction

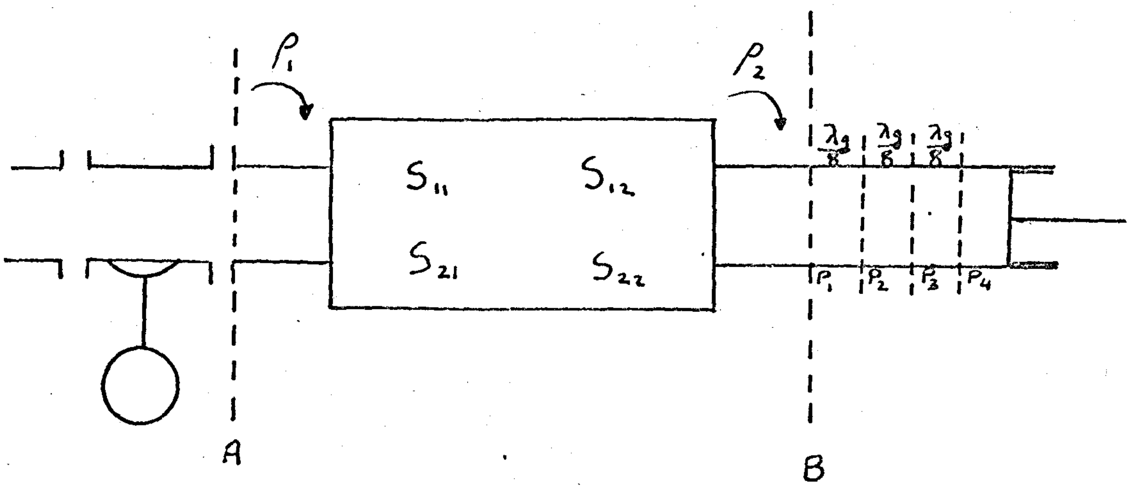

FIGURE 3.2: Experimental Set-up

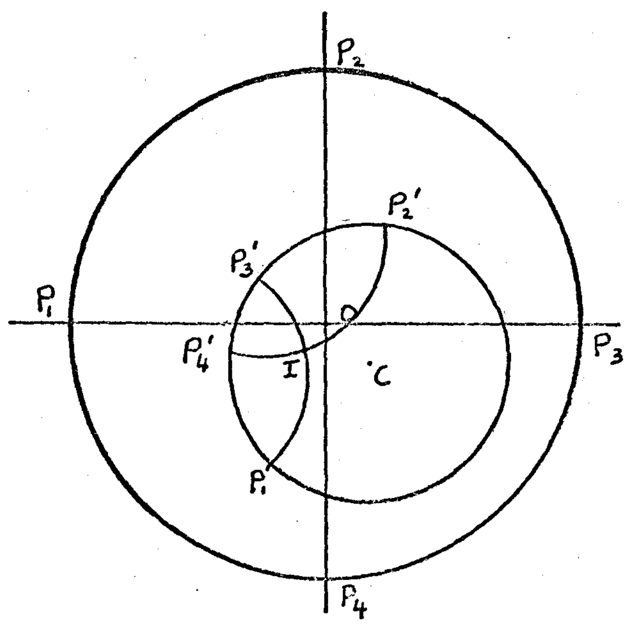

FIGURE 3.3: The Unit Circle and its Image

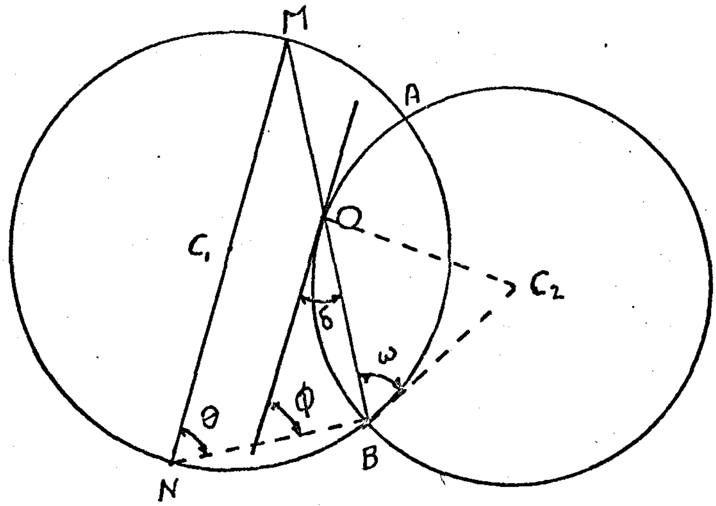

FIGURE 3.4: Proof of Theorem

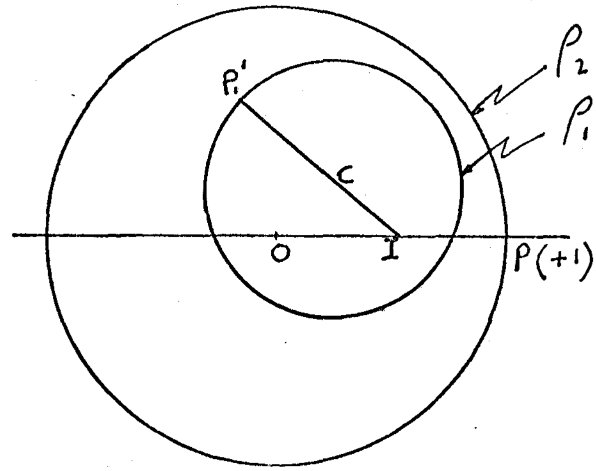

FIGURE 3.5: Unit Circle and its Image with arg. S_{11} = arg. S_{22} = 0

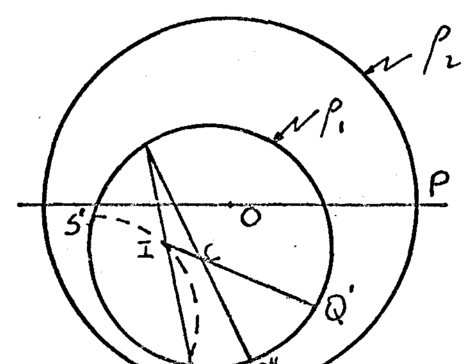

FIGURE 3.6: Scattering Parameters of the Junction

The schematic diagram of a high precision reflection bridge is shown in Figure 3.7. The microstrip transmission line is connected to one side arm and the precision short and attenuator in the other are adjusted until the output is minimized.

The hybrid "tee" is converted into a magic "tee" by inserting slide screw tuners in the E, H and side arms to compensate for asymmetry. The magic "tee" has the property that when the reflection coefficients at the reference planes in the side arms are equal, the power fed to the detector in the E arm is zero.

The reflection coefficient at a measuring plane of the sample arm of the hybrid tee which contains the microstrip line

$$\rho(x) = \rho_2 e^{2\gamma s \ell s} \tag{3.13}$$

where ρ_2 = reflection coefficient at port 2.

γ_s = propagation constant in the sample arm.

ℓ_s = distance of measuring plane from port 2.

For a hybrid "tee"

$$b = Sa$$

or

$$\begin{bmatrix} b_1 \\ b_2 \\ b_3 \\ b_4 \end{bmatrix} = \begin{bmatrix} S_{11} & S_{12} & S_{13} & S_{14} \\ S_{21} & S_{22} & S_{23} & S_{24} \\ S_{31} & S_{32} & S_{33} & S_{34} \\ S_{41} & S_{42} & S_{43} & S_{44} \end{bmatrix} \begin{bmatrix} a_1 \\ a_2 \\ a_3 \\ a_4 \end{bmatrix} \tag{3.14}$$

where a = incident wave

b = scattered wave

S = scattering matrix

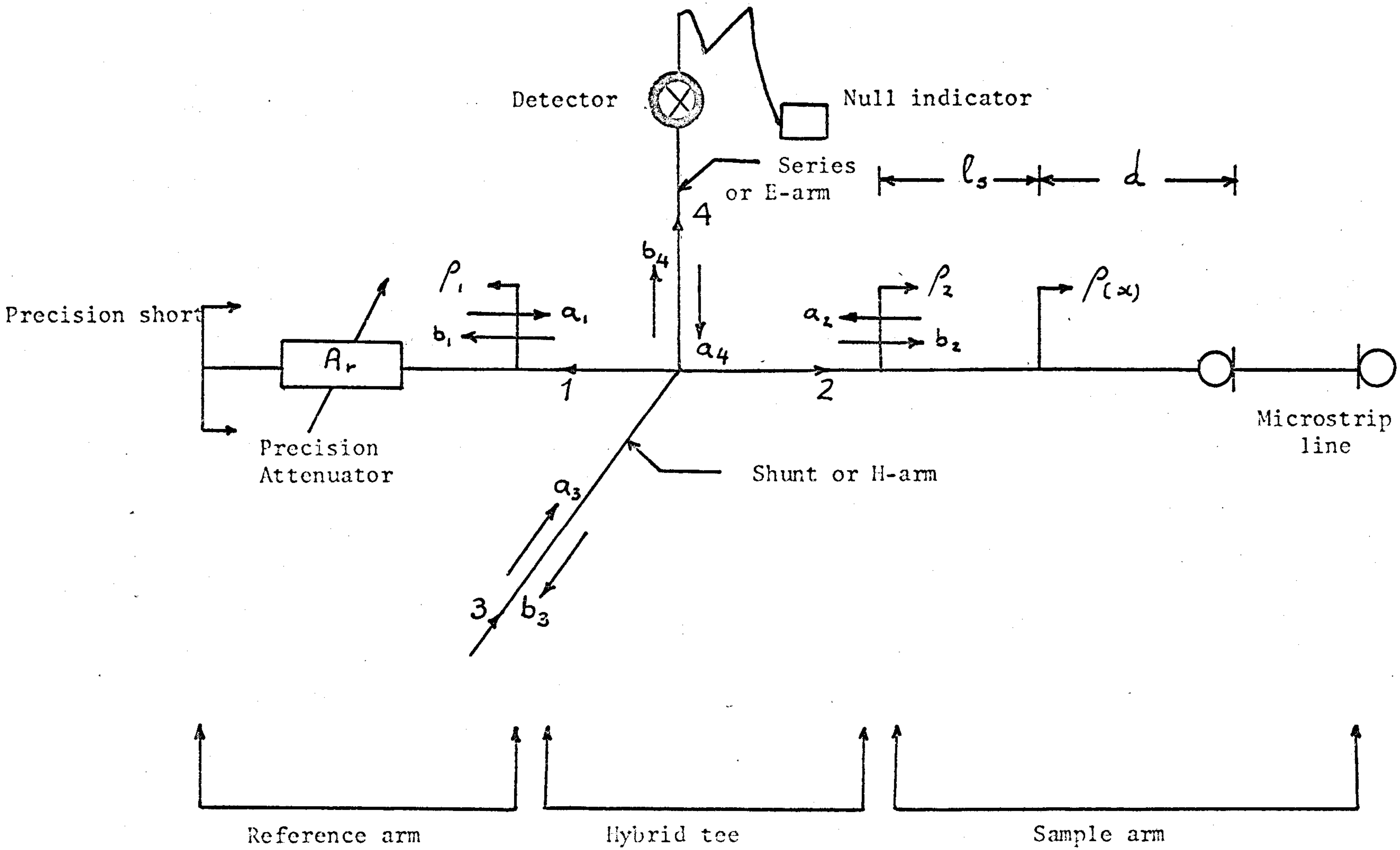

FIGURE 3.7: A Microwave Reflection Bridge

Because of receprocity, S is symmetrical, i.e. $S_{12} = S_{21}$, $S_{13} = S_{31}$ --- etc.

The reflection coefficients

$$\left.\begin{aligned} \rho_1 &= \frac{a_1}{b_1} \\ \text{and} \quad \rho_2 &= \frac{a_2}{b_2} \\ \text{The null condition is } a_4 &= b_4 = 0 \end{aligned}\right\} \quad (3.15)$$

Solving equations (3.13), (3.14) and (3.7) gives

$$\rho(x) = \frac{\rho_1 \, a - b}{\rho_1 \, c - 1} \quad (3.16)$$

where

$$a = \left[\frac{S_{11} \, S_{34} - S_{13} \, S_{14}}{S_{22} \, S_{34} - S_{23} \, S_{24}}\right] e^{2\gamma_s \ell_s} \quad (3.16a)$$

$$b = \left[\frac{S_{34}}{S_{22} \, S_{34} - S_{23} \, S_{24}}\right] e^{2\gamma_s \ell_s} \quad (3.16b)$$

and

$$c = \frac{[(S_{11}S_{22} - S_{12}^{\;2})S_{34} + (S_{13}S_{12} - S_{23}S_{11})S_{24} + (S_{12}S_{23} - S_{13}S_{22})S_{14}]}{S_{22}S_{34} - S_{23}S_{24}}$$

------------- (3.16c)

The reflection coefficient ρ_1 of the reference arm has been shown by Champlin, K. S. et. al[26] to be equal to:

$$\rho_1 = Ke^{-2(A_r + j\beta_r \ell_r)} \quad (3.17)$$

where

$K = K_A K_S$

K_A = residual attenuation of the attenuator

K_S = zero setting and fixed loss of short circuit.

A_r = reading of precision attenuator in nepers.

$\beta_r \ell_r$ = reading of precision short in radians.

Equation (3.16) reduces to:

$$\rho(x) = \frac{Ae^{-2(A_r + j\beta_r \ell_r)} - B}{Ce^{-2(A_r + j\beta_r \ell_r)} - 1} \tag{3.18}$$

where

$A = aK$

$B = b$

$C = cK$

Equation (3.18) gives the general expression for the reflection coefficient of the microstrip line. The constants A, B, and C can be determined by preliminary measurements, which results in the calibration of the bridge.

(1) Bridge Calibration -

(i) The Matched and Symmetric Bridge:

When the bridge is matched and compensated for asymmetry, then

$S_{11} = S_{22}$, $S_{13} = S_{23}$, $S_{14} = -S_{24}$, and $S_{34} = S_{43} = 0$

Under these conditions, from equations (3.16b) and (3.16c),

$B = 0$, $C = 0$

and equation (3.18) reduces to:

$$(x) = -Ae^{-2(A_r + j\beta_r \ell_r)} \tag{3.19}$$

The coefficient A can be determined experimentally by balancing the bridge with a fixed short circuit terminating the sample arm.

When a precision short circuit is placed at d_1,

$$\rho(S_1) = \rho(x)e^{2\gamma_s d_1}$$

or

$$-1 = \rho(x)e^{2\gamma_s d_1}$$

$$\therefore \rho(x) = -e^{-2\gamma_s d_1}$$

From equation (3.19)

$$-e^{-2\gamma_s d_1} = -Ae^{-2(A_r(S_1) + j\beta_r \ell_r(S_1))}$$

where

$A_r(S_1)$ = attenuation reading with a fixed short.

$\beta_r \ell_r$ = precision short reading with a fixed short.

or

$$A = \frac{e^{-2\gamma_s d_1}}{e^{-2(A_r(S_1) + j\beta_r \ell_r(S_1))}}$$

Therefore, by substituting in equation (3.19),

$$\rho(x) = e^{-2[(A_r - A_r(S_1)) + j\beta_r(\ell_r - \ell_r(S_1) + d_1)]}$$

$$= e^{-(A + j\phi)} \qquad (3.20)$$

where

$$A = 2[A_r - A_r(S_1)] \text{ in nepers} \qquad (3.20a)$$

$$\phi = 2\beta_r[\ell_r - \ell_r(S_1) + d_1] \text{ in radians} \qquad (3.20b)$$

Equation (3.20) has been used for the practical measurement of the magnitude and phase of the reflection coefficients at the waveguide-microstrip line junction.

(ii) The matched and unsymmetric bridge:

If the input ports of a hybrid "tee" are matched and the bridge is not compensated for asymmetry, then,

$$S_{11} = S_{22} = 0$$

$$S_{12} = S_{21} = 0 \text{ at a single frequency}$$

And since by equation (3.16c) C = 0, then

$$\rho(x) = -Ae^{-2(A_r + j\beta_r\ell_r)} + B \tag{3.21}$$

With a precision short circuit termination at the sample arm,

$$-e^{-\gamma_s d_1} = -Ae^{-2(A_r(S_1) + j\beta_r\ell_r(S_1))} + B \tag{3.21a}$$

With a matched termination Z_o at the sample arm,

$$0 = -Ae^{-2[A_r(Z_o) + j\beta_r\ell_r(Z_o)]} + B \tag{3.21b}$$

Therefore, solving equations (3.21a) and (3.21b) for A and B, and substituting in equatinn (3.21) gives

$$\rho(x) = \frac{-e^{-2\gamma_s d_1}}{\left[1 - \frac{\rho_1(Z_o)}{\rho_1(S_1)}\right]} \left[e^{-2(A_r - A_r(S_1) + j\beta_r(\ell_r - \ell_r(S_1)))}, - \frac{\rho_1(Z_o)}{\rho_1(S_1)}\right] \qquad \text{----------} \quad (3.22)$$

where

$$\frac{\rho_1(Z_o)}{\rho_1(S_1)} = \frac{e^{-2[A_r(Z_o) + j\beta_r\ell_r(Z_o)]}}{e^{-2[A_r(S_1) + j\beta_r\ell_r(S_1)]}}$$

Therefore $\rho(x)$ can be evaluated using equation (3.22).

(iii) <u>The general bridge</u>:

The reflection coefficient of a general bridge is given by equation (3.18) with A, B and C being constants of the bridge. These three constants can be determined by calibrating the bridge with two shorts at two different distances d_1 and d_2 from the measuring plane and with one matched termination Z_o at the sample arm.

CHAPTER IV

EXPERIMENTAL PROCEDURES

4.1 PREPARATION OF THE TEST SAMPLES:

Germanium substrates in the form of rectangular slices 2" long, 3/4" wide and having thicknesses varying between 24 and 57 mils were cut from a large block of intrinsic Ge <111> crystal by means of a 20 mil diamond head wheel cutter. The slices were then carefully polished by hand with silicon carbide paper and their thicknesses accurately measured with a Moore and Wright micrometer screw gauge. Before proceeding to deposit the film conductors, the substrates were carefully washed using a commercial cleaner, methyl alcohol and finally distilled water. This was done by means of a Heat Systems Co. Automatic Cleaner, Model HD-50.

A substrate holder able to firmly hold the thin Ge slices was machined from aluminum, and appropriate masks having 2" slots of varying widths were made from 20 mils shimstock steel sheets.

Thus using the coating unit described below, the substrate holder and the shimstock steel masks, one side of the thin Ge slices was completely metalized, while on the other side conducting strips of varying widths were deposited. Both silver and aluminum were evaporated to produce the conducting films.

The Coating Unit -

An Edwards model 12E3 vacuum-coating unit was employed in the production of the thin conducting films. The unit has a liquid nitrogen trap in the form of a spirally wound length of 3/8" copper tubing at the throat of the diffusion pump to reduce backstreaming of the diffusion pump oil and to condense water and other vapours present. A vacuum of approximately 1×10^{-6} torr was obtainable, although most evaporations were made in a vacuum of $\lesssim 8 \times 10^{-5}$ torr.

This coating unit has a 12" bell jar with a four position rotary filament holder to allow successive evaporations without breaking vacuum. Tungsten helical coils were used as filaments for the evaporation of aluminum to produce minimum contamination in the Al films deposited, while molybdenum boats were used for the evaporation of silver.

Since silver and aluminum have conductivities of 6.17×10^7 and 3.54×10^7 mhos/m respectively, their respective skin depths at 9.38 GHz will be approximately 0.66 and 0.88 microns respectively. To obtain good microstrip lines of minimum conductor losses requires the conductor layer to be more than 3 skin depths thick. So using the method reported by R. Dynes[27], care was taken to ensure that the conductor layers were more than 3.00 microns thick.

The strip conductor widths were measured by a Bauch and Lomb 10"-optical comparator.

4.2 DESCRIPTION OF APPARATUS:

A schematic diagram of a reflection bridge for the precision measurement of the magnitude and phase of the reflection coefficient at the waveguide-microstrip junction is shown in Figure 4.1. The equipment used is as follows: -

(i) Klystron

The klystron used as a signal source is an X-13 reflex type of Varian Associates of Canada Ltd. Its frequency is mechanically tunable over a range of 8.2 - 12.4 GHz, and its maximum power output for optimum load is 350 mw.

The power to the klystron was supplied from a PRD power supply type 890A. The reflector voltage can be modulated either from an external source or an internally produced square and sawtooth waves.

(ii) Ferrite Isolators

An unidirectional element is used to isolate the klystron from the rest of the circuit. For transmission in the forward direction, the isolator has virtually zero attenuation, while for the reverse direction, it introduces approximately 30db attenuation. The isolators used in the bridge were manufactured by PRD.

(iii) Wave Meter

The wavemeter used was a Micro-line, model 138A. This meter reads the frequency of the waves in the guide in the frequency range 8.430 - 9.660 GHz.

(iv) Variable Attenuator

This is used to adjust the power input to the circuit, and a PRD unit was used.

(v) Standing Wave Indicator

The standing wave indicator is a model B433 (1637) of Elliott Brothers (London) Ltd. and is a high precision instrument. It has been used for the measurement of the V.S.W.R. during the matching of the hybrid "tee" ports by means of the tuners.

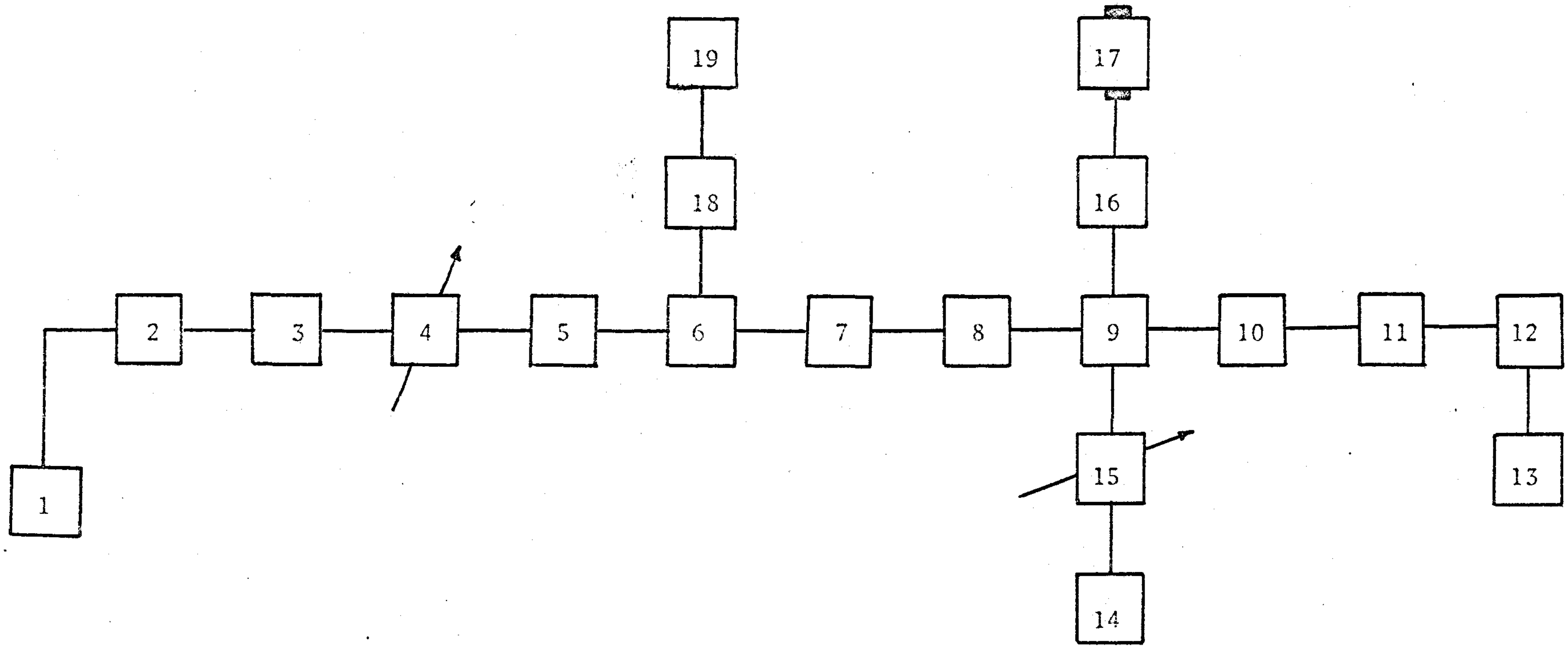

1. Klystron Power Supply
2. Klystron
3, 11. Isolators
4. Attenuator
5. Wave Meter
6. Directional Wave Indicator
8, 10, 16. Stub Tuners
9. Hybrid Tee
12. Crystal Detector
7. Standing Wave Indicator

13. D.C. Micro Volt-Ammeter
14. Precision Short
15. Precision Rotary Attenuator
17. Microstrip Jig
18. Crystal Detector
19. Indicator

FIGURE 4.1: Experimental Set-up of the Reflection Bridge

(vi) Hybrid Tee, Precision Attenuator and Precision Short

High quality equipment is needed for these components to avoid undesirable reflections. Elliott instruments were used for the attenuator and short circuit, while the hybrid tee was manufactured by Demornay Bonardi.

(vii) Microstrip Line Jig

A jig for testing 2" long microstrip transmission lines was machined from brass. Two 50-ohm OSM244-3 (Two-Hole, Flange Mount, Jack/Tab) connectors were fixed on the walls at both ends of the jig. The walls were allowed to be moved in the vertical direction, thus enabling the 50 mil centre conductor of the miniature connectors to be adjusted to extend over and firmly touch the ends of the strip conductor.

One of the OSM coaxial-to-microstrip transitions was connected to a series coaxial adapter Model 21020 N Plug/OSM Jack and a Hewlett-Packard Adapter, model X281B waveguide/N Jack. This then, constituted the waveguide to microstrip lossy junction whose scattering parameters were not known, and had to be experimentally determined.

4.3 MEASUREMENT PROCEDURES:

The measurements were made at a frequency of 9.38 GHz. This gives a free space wavelength of 3.20 cm which is divisable by 8, thus facilitating the implementation of the Deschamps method.

The setting up procedure was as follows: -

Referring to Figure 4.1 the ports 1, 2 and 4 were terminated in matched loads and S_{33} was made minimum (obtaining a VSWR of less than 1.02) using the tuner in arm 3. Then S_{34} was made minimum by using the tuner in arm 2, the ports 1, 2 and 4 still being terminated in matched loads.

Then by feeding arm 2 and terminating the other ports in matched loads, S_{22} and S_{12} were simultaneously made minimum using the tuner in arm 4. These conditions make $S_{44} = 1$, thus compensating for the asymmetry in the hybrid tee. The performance of the bridge was then described by equation (3.20) and it was ready for measurement.

4.3.1 Determination of the Scattering Parameters of the Waveguide-Microstrip Junction

In order to apply the measurement technique described in Chapter III, a 50-ohm microstrip line on air dielectric was built using 10 mil thick copper sheets as the conductor. The strip conductor was carefully cut and finely polished to give a strip approximately 150 mils wide and 1.6 cm. long ($\lambda g/2$). The air dielectric was fixed to have a thickness of approximately 27 mils giving $W/h \cong 5.5$, i.e. $Z_o = 50$ ohms. A large copper slab was soldered to the strip conductor to provide a good short circuit between the strip conductor and the ground plane of the microstrip line.

The sample arm was first shorted by a fixed short circuit plate and the precision attenuator and the precision short were then adjusted for minimum output. Their readings A_o and ℓ_o were recorded. The short was then replaced by the unknown waveguide-microstrip junction, with the tab of the OSM connector extending over and contacting the shorted 50-ohm microstrip line on air dielectric. Again, the precision attenuator and the precision short were adjusted for minimum output, and their readings A_1 and ℓ_1 recorded. The line was then carefully cut by 0.4 cm ($\lambda g/8$) and the corresponding precision attenuator and short positions to give a minimum output noted. By repeating this procedure for four points, and plotting the reflection coefficients on a polar graph, the scattering parameters of the unknown junction were determined. This experiment was repeated about twenty times until accurate values of the parameters were ensured.

Now that the scattering parameters of the lossy junction were determined, a well-known method[28] of finding transmission-line characteristic impedance is to measure the short-circuit and open-circuit input impedances and then calculate Z_o from:

$$Z_o = \sqrt{Z_{sc} Z_{oc}}$$

The air-dielectric microstrip line was replaced by the fabricated microstrip lines on germanium substrates, and the precision attenuator and the precision short were adjusted for minimum output when the lines were terminated in open circuits and short circuits. With the aid of the digital computer, the true characteristic impedances of the microstrip lines were calculated.

4.4 MEASUREMENT OF THE D.C. RESISTIVITY OF THE SUBSTRATE:

The conductivity of the semiconductor substrate was measured by the four point probe method which has the advantage that it does not require any specific shape of the sample.

In this method, four probes are placed on the flat surface of the sample and current I is passed through the outer probes and the voltage V is measured between the inner probes. Then the conductivity σ is given by[29]:

$$\sigma = \frac{1}{2\pi V}\left[\frac{1}{S_1} + \frac{1}{S_3} + \frac{1}{S_1+S_2} - \frac{1}{S_1+S_3}\right] \tag{4.1}$$

where S_1, S_2 and S_3 are the probe spacings.

When the probe spacings are equal, the resistivity ρ is given by:

$$\rho = 2\pi S \frac{V}{I} \qquad (4.2)$$

Equation (4.2) was used to calculate the D.C. resistivity of the Ge substrate and it was found to be 47.4 ohm-cm at room temperature ($T \cong 300°K$). Since the dimensions of the slices were large compared to the probe spacings, no corrections were applied.

CHAPTER V

RESULTS

5.1 THEORETICAL RESULTS:

5.1.1 Conformal Transformation Method

The characteristic impedance of microstrip transmission lines on intrinsic germanium substrates based on a Schwarz-Chirstoffel transformation method is plotted vs. w/h in Figure 5.1. Equations 2.16(a) and 2.16(b) were numerically solved on an IBM 7040 digital computer using the Newton-Raphson method, and the characteristic impedance Z_o was calculated from Equation 2.15. It was found, however, that the approximate expression for Z_o given in equation 2.17 gave good results for values of $w/h > 2$.

The conformal transformation solution is compared with Wheeler's solution in Figure 5.1, and it can be seen that close agreement is obtained for values of $w/h > 0.6$.

5.1.2 Variational Method

(a) Microstrip lines with negligible strip thickness -

The line capacitance, characteristic impedance and guide wavelength of microstrip lines on silicon and germanium substrates have been calculated as a function of w/h, using Equations 2.37, 2.20(a) and 2.20(b). All integrations have been carried out on an IBM 7040 digital computer using Simpson's rule.

The calculated values of C/ε_o, Z_o and λ/λ_o are shown in Table 5.1 and are given in graphical form in Figures 5.2(a), 5.2(b) and 5.2(c).

FIGURE 5.1: Comparison Between Conformal Transformation Solution and Wheeler's Solution for Microstrip Lines on Intrinsic Germanium Substrates

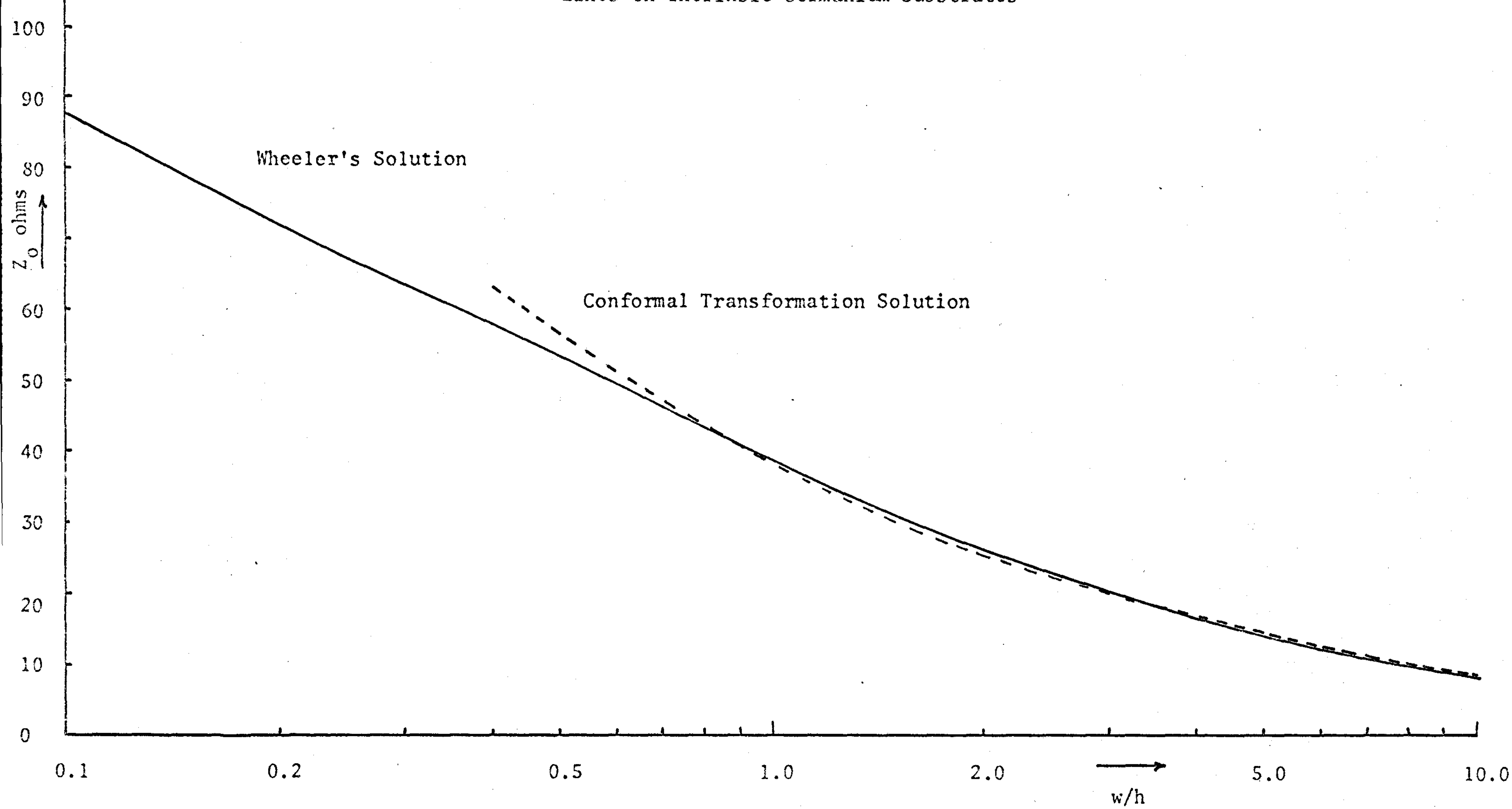

(b) Microstrip lines with finite strip thickness -

The line capacitance, characteristic impedance and guide wavelength of microstrip lines on germanium substrates have been computed as a function of both w/h and t/h. They are shown in Table 5.2 and are given in graphical form in Figures 5.3(a), 5.3(b) and 5.3(c).

(c) Microstrip lines on two dielectric layer substrates with negligible strip thickness -

The line capacitance, characteristic impedance and guide wavelength of microstrip lines on two dielectric layer substrates ($\varepsilon_1 = 16.0$, $\varepsilon_2 = 7.0$) have been computed as a function of w/h and b/h from Equations 2.48, 2.20(a), and 2.20(b). They are shown in Table 5.3 and are given in graphical form in Figures 5.4(a), 5.4(b) and 5.4(c).

(d) Microstrip lines on two-dielectric layer substrates with finite strip thickness -

The line capacitance, characteristic impedance and guide wavelength of microstrip lines on two dielectric layer substrates ($\varepsilon_1 = 16.0$, $\varepsilon_2 = 7.0$) have been computed as a function of w/h and b/h for a value of t/h = 0.05 using Equations 2.53, 2.20(a) and 2.20(b). They are shown in Table 5.4 and given in graphical form in Figures 5.5(a), 5.5(b) and 5.5(c).

5.1.3 Losses in Microstrip Lines on Germanium Substrates

The total calculated losses incurred in microstrip lines on intrinsic Germanium substrates at room temperature ($\rho \approx 47.2$ ohm-cm) and at T = 240°K ($\rho \approx 2000$ ohm-cm) are shown in Table 5.5. It is to be noted that in both cases the substrate loss is predominant.

The calculations have been carried out on the microstrip lines whose characteristic impedances were experimentally measured.

TABLE 5.1

Line Capacitance, Characteristic Impedance and Guide Wavelength of Microstrip Lines of Negligible Strip Thickness

w/h	$\varepsilon_r = 1.0$		$\varepsilon_r = 11.7$			$\varepsilon_r = 16.0$		
	c_o/ε_o	Z_o	c/ε_o	Z_o	λ/λ_o	c/ε_o	Z_o	λ/λ_o
0.1	1.450	260	10.14	98.31	.3780	13.62	84.83	.3262
0.4	2.058	183	15.03	67.79	.3700	20.22	58.45	.3190
0.7	2.507	150	18.88	54.80	.3644	25.43	47.22	.3140
1.0	2.902	120	22.42	46.74	.3598	30.22	40.25	.3099
1.3	3.270	115	25.82	41.03	.3559	34.83	35.32	.3064
1.6	3.621	104.2	29.12	36.71	.3526	39.32	31.59	.3035
1.9	3.960	95	32.36	33.31	.3498	43.71	28.66	.3010
2.2	4.288	87.8	35.52	30.55	.3474	48.01	26.28	.2989
2.5	4.608	81.6	38.62	28.26	.3454	52.22	24.30	.2971
2.8	4.921	76.6	41.66	26.33	.3437	56.34	22.64	.2955
3.1	5.226	72	44.64	24.68	.3422	60.39	21.22	.2942
3.4	5.527	68	47.57	23.25	.3409	64.38	19.99	.2930
3.7	5.822	64.7	50.45	22.00	.3397	68.30	18.91	.2920
4.0	6.113	61.5	53.30	20.89	.3387	72.16	17.95	.2911
4.3	6.400	58.8	56.11	19.89	.3377	75.98	17.10	.2902
4.6	6.683	56.5	58.89	19.00	.3369	79.76	16.33	.2895
4.9	6.963	54.2	61.64	18.20	.3361	83.50	15.63	.2888
5.2	7.240	52.0	64.38	17.46	.3354	87.22	15.00	.2881
5.5	7.514	50	67.09	16.79	.3347	90.91	14.42	.2875
5.8	7.786	48.5	69.79	16.17	.3340	94.58	13.89	.2869
6.1	8.056	47.4	72.48	15.60	.3334	98.24	13.40	.2869
7.4	9.203	40.98	84.03	13.56	.3309	113.95	11.64	.2842
8.7	10.32	36.6	95.48	12.01	.3288	129.54	10.31	.2823
10.0	11.42	33.0	106.90	10.79	.3269	145.10	9.26	.2806

FIGURE 5.2(a) Line Capacitance of Microstrip Lines as a Function of w/h

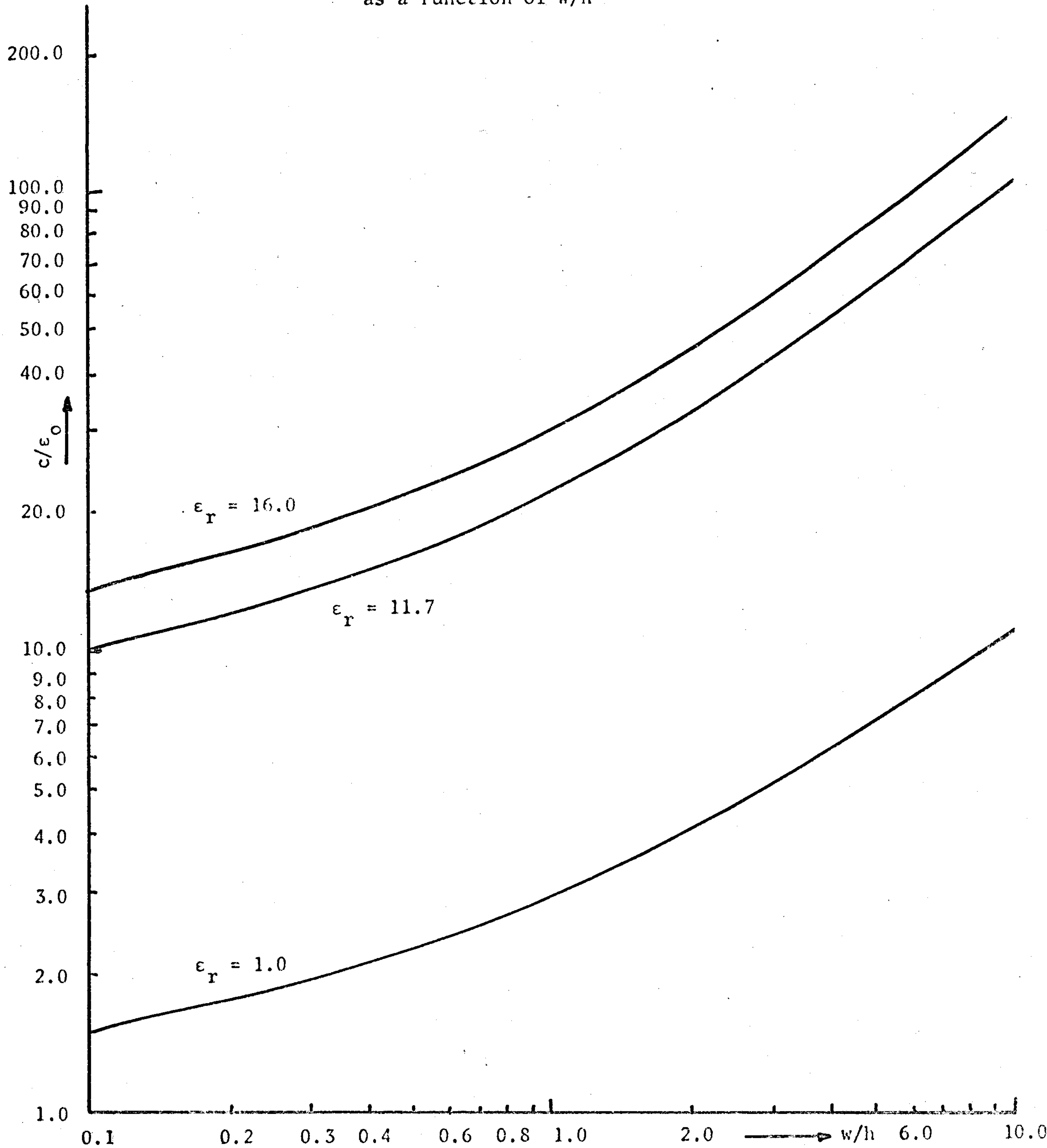

FIGURE 5.2(b): Characteristic Impedance of Microstrip Lines with Negligible Conductor Thickness

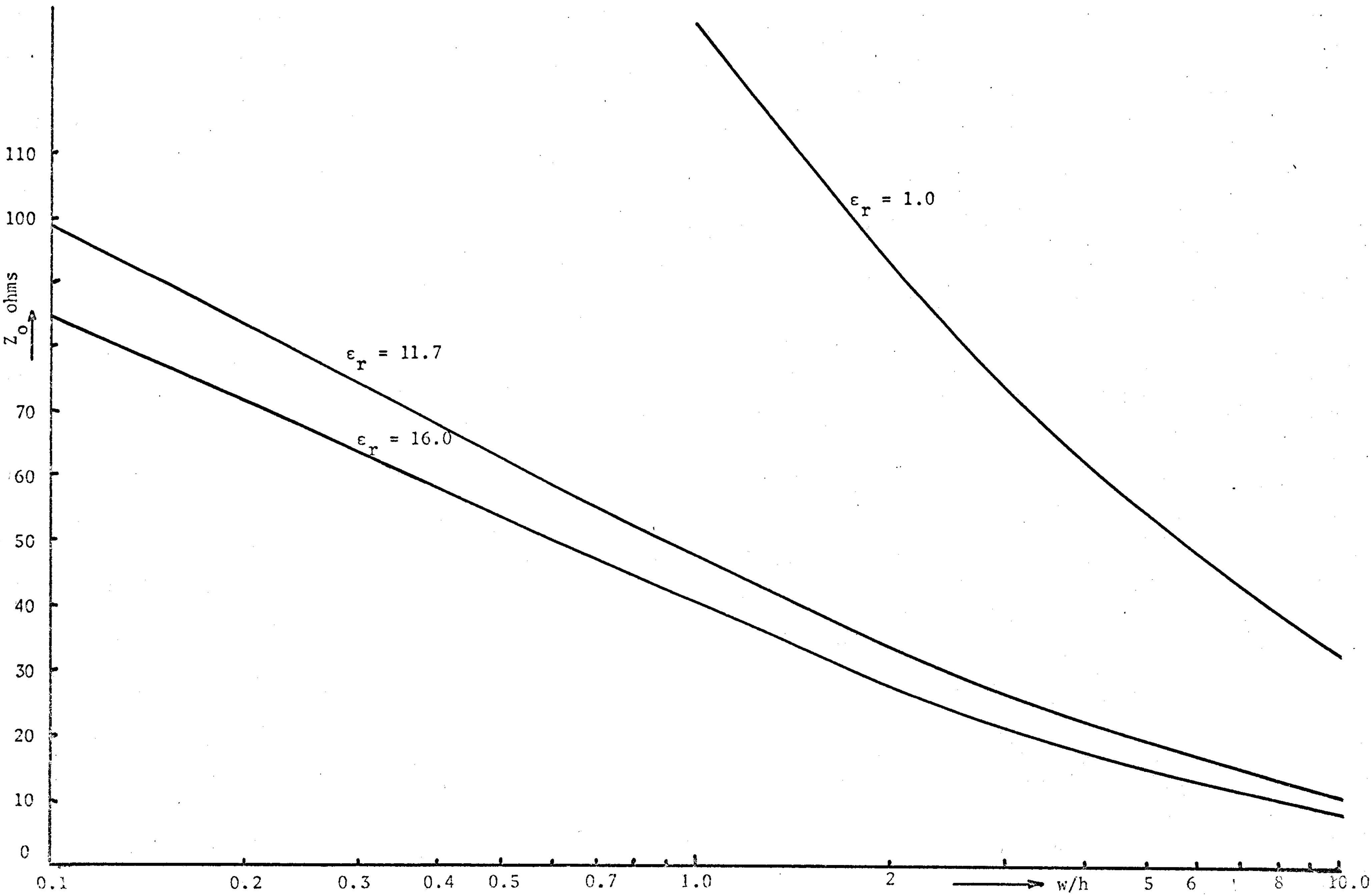

FIGURE 5.2(c): Guide Wavelength of Microstrip Lines as a Function of w/h

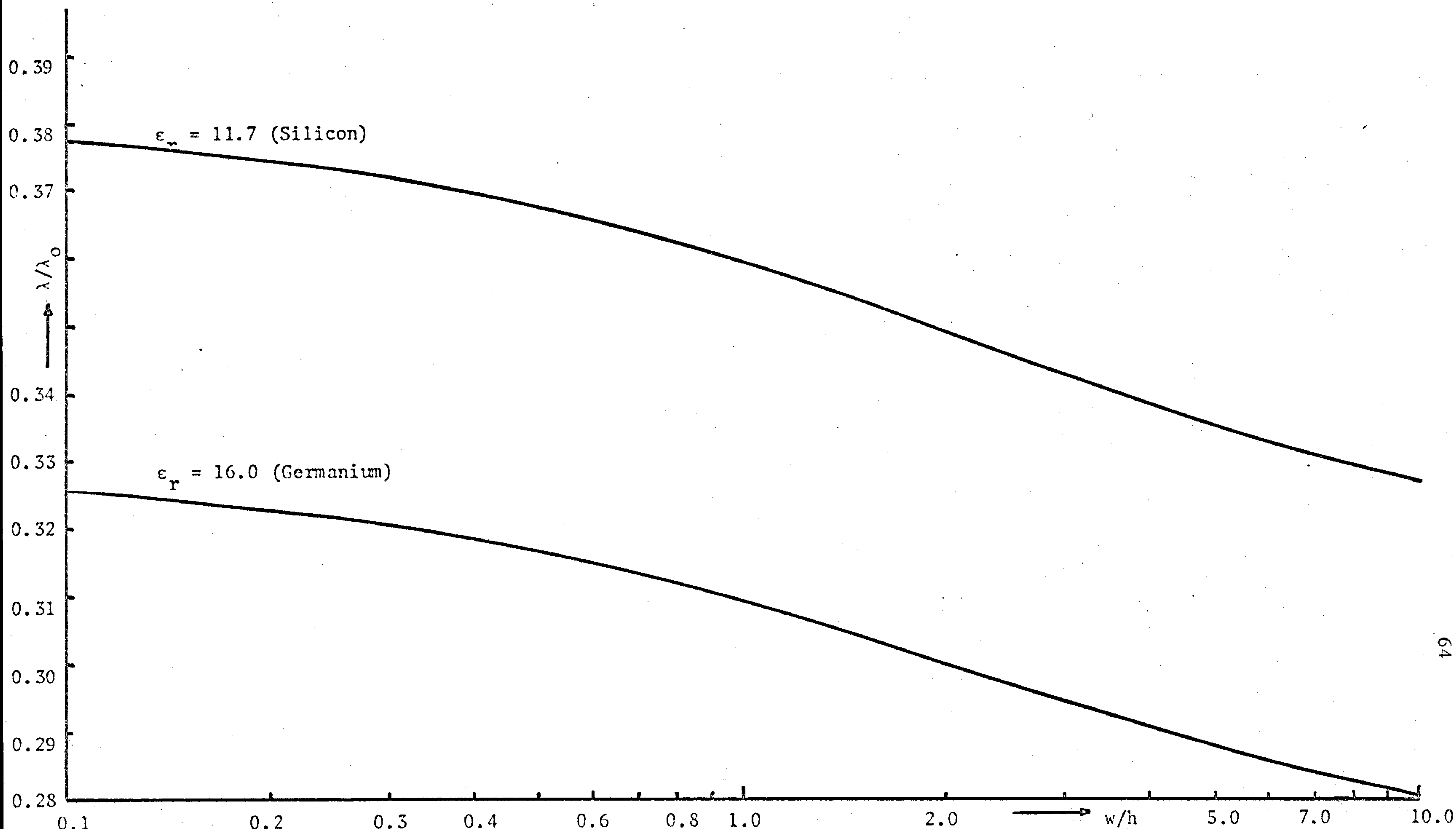

TABLE 5.2

Line Capacitance, Characteristic Impedance and Guide Wavelength of Microstrip of Finite Strip Thickness on Intrinsic Germanium Substrate (ϵ_r=16.0)

w/h	t/h = 0.02				t/h = 0.04			
	c_o/ϵ_o	c/ϵ_o	Z_o	λ/λ_o	c_o/ϵ_o	c/ϵ_o	Z_o	λ/λ_o
0.1	1.529	14.45	80.19	.3253	1.591	15.91	76.92	.3246
0.4	2.114	20.86	56.78	.3184	2.162	21.40	55.43	.3179
0.7	2.555	26.01	46.25	.3134	2.599	26.52	45.41	.3130
1.0	2.947	30.79	39.58	.3094	2.989	31.30	38.98	.3090
1.3	3.313	35.39	34.81	.3060	3.354	35.91	34.35	.3056
1.6	3.664	39.89	31.18	.3031	3.704	40.41	30.82	.3028
1.9	4.003	44.29	28.31	.3006	4.043	44.82	28.01	.3003
2.2	4.333	48.60	25.98	.2986	4.372	49.14	25.72	.2983
2.5	4.656	52.83	24.04	.2969	4.695	53.38	23.81	.2966
2.8	4.973	56.98	22.40	.2954	5.012	57.54	22.20	.2951
3.1	5.285	61.07	20.98	.2942	5.325	61.64	20.81	.2939
3.4	5.595	65.09	19.75	.2932	5.635	65.68	19.66	.2929
3.7	5.903	69.09	18.67	.2923	5.943	69.68	18.53	.2921
4.0	6.211	73.05	17.69	.2916	6.252	73.66	17.57	.2913
4.3	6.521	77.02	16.82	.2910	6.562	77.64	16.70	.2907
4.6	6.835	81.03	16.02	.2904	6.877	81.66	15.91	.2902
4.9	7.157	85.12	15.27	.2900	7.200	85.76	15.17	.2897
5.2	7.492	89.38	14.57	.2895	7.536	90.04	14.47	.2893
5.5	7.848	93.92	13.89	.2891	7.893	94.62	13.79	.2888
5.8	8.236	98.97	13.20	.2885	8.284	99.70	13.118	.2882
6.1	8.682	104.96	12.49	.2876	8.732	105.74	12.41	.2874

(CONTINUED)

TABLE 5.2

Line Capacitance, Characteristic Impedance and Guide Wavelength of Microstrip of Finite Strip Thickness on Intrinsic Germanium Substrates (ε_r=16.0)

t/h = 0.06				t/h = 0.08				t/h = 0.10			
c_o/ε_o	c/ε_o	Z_o	λ/λ_o	c_o/ε_o	c/ε_o	Z_o	λ/λ_o	c_o/ε_o	c/ε_o	Z_o	λ/λ_o
1.642	15.64	74.38	.3241	1.687	16.11	72.31	.3236	1.727	16.53	70.57	.3232
2.205	21.87	54.29	.3175	2.243	22.30	53.30	.3171	2.278	22.70	52.42	.3168
2.639	27.00	44.67	.3127	2.676	27.42	44.01	.3123	2.716	27.83	43.42	.3121
3.027	31.77	38.44	.3087	3.063	32.21	37.96	.3084	3.097	32.62	37.51	.3081
3.392	36.39	33.94	.3053	3.428	36.84	33.55	.3050	3.462	37.26	33.19	.3048
3.741	40.90	30.48	.3025	3.777	41.36	30.16	.3022	3.811	41.80	29.87	.3020
4.079	45.31	27.73	.3000	4.116	45.79	27.46	.2998	4.150	46.24	27.21	.2996
4.410	49.65	25.49	.2980	4.446	50.14	25.25	.2978	4.480	50.61	25.04	.2976
4.733	53.90	23.60	.2963	4.769	54.40	23.41	.2961	4.804	54.89	23.22	.2959
5.506	58.08	22.01	.2949	5.087	59.59	21.84	.2947	5.122	59.08	21.67	.2944
5.364	62.18	20.64	.2937	5.400	62.71	20.49	.2935	5.436	63.22	20.34	.2933
5.674	66.24	19.45	.2927	5.711	66.77	19.31	.2925	5.747	67.29	19.17	.2923
5.983	70.25	18.39	.2918	6.020	70.80	18.26	.2916	6.057	71.33	18.14	.2914
6.292	74.24	17.44	.2911	6.330	74.80	17.33	.2909	6.367	75.35	17.21	.2907
6.602	78.23	16.59	.2905	6.641	78.80	16.48	.2903	6.679	79.37	16.37	.2896
6.918	82.27	15.80	.2900	6.958	82.86	15.70	.2898	6.997	83.44	15.60	.2896
7.249	86.39	15.07	.2895	7.283	87.00	14.98	.2983	7.322	87.60	14.89	.2891
7.578	90.69	14.38	.2891	7.621	91.32	14.29	.2889	7.662	91.94	14.20	.2887
7.938	95.29	13.71	.2886	7.981	95.95	13.62	.2884	8.023	96.59	13.54	.2882
8.329	100.42	13.04	.2881	8.374	101.1	12.96	.2878	8.418	101.8	12.88	.2876
8.780	106.5	12.33	.2871	8.827	107.24	12.25	.2870	8.873	108.0	12.18	.2867

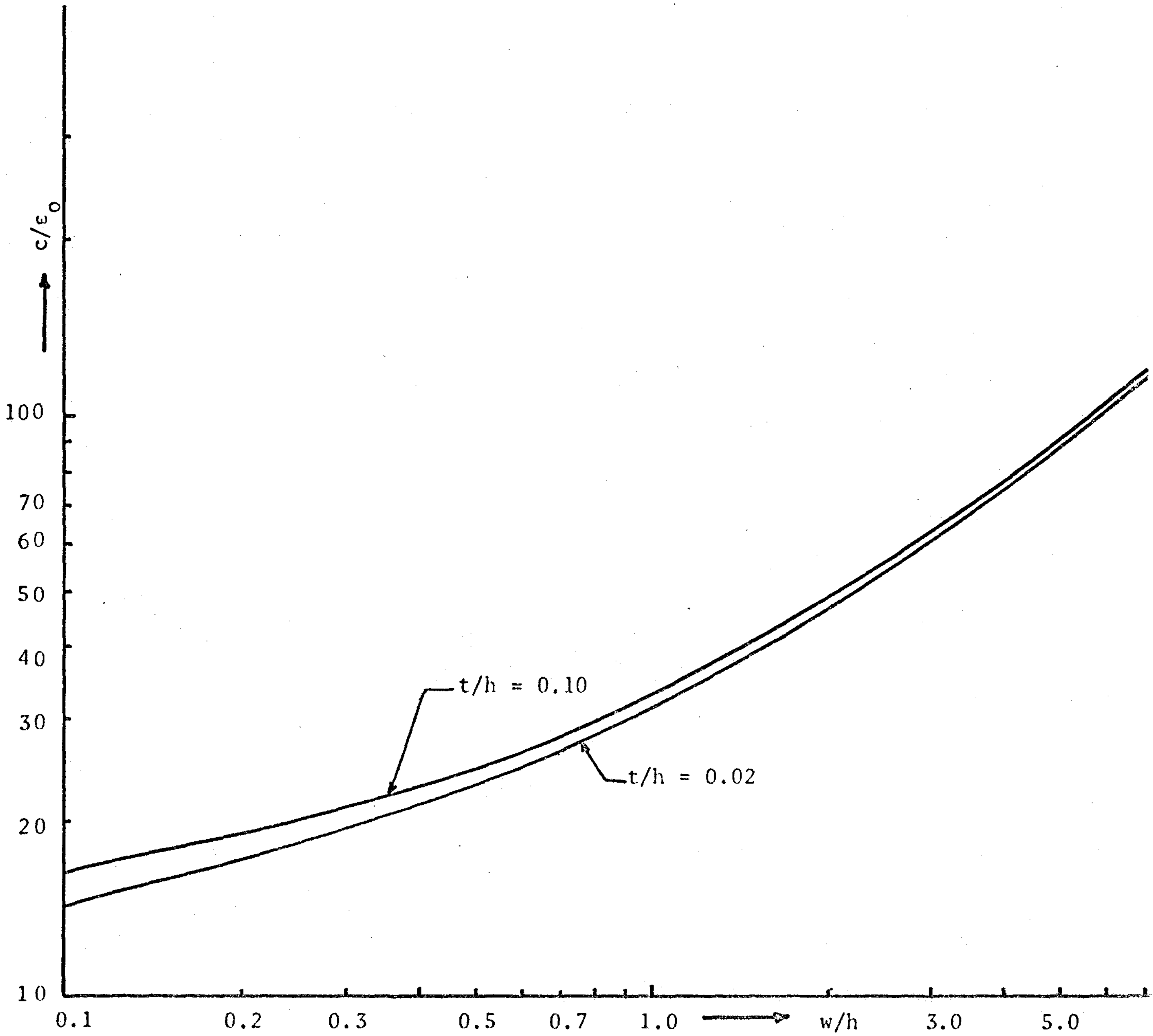

FIGURE 5.3(a): Line Capacitance of Microstrip Lines of Finite Strip Thickness on Ge Substrates

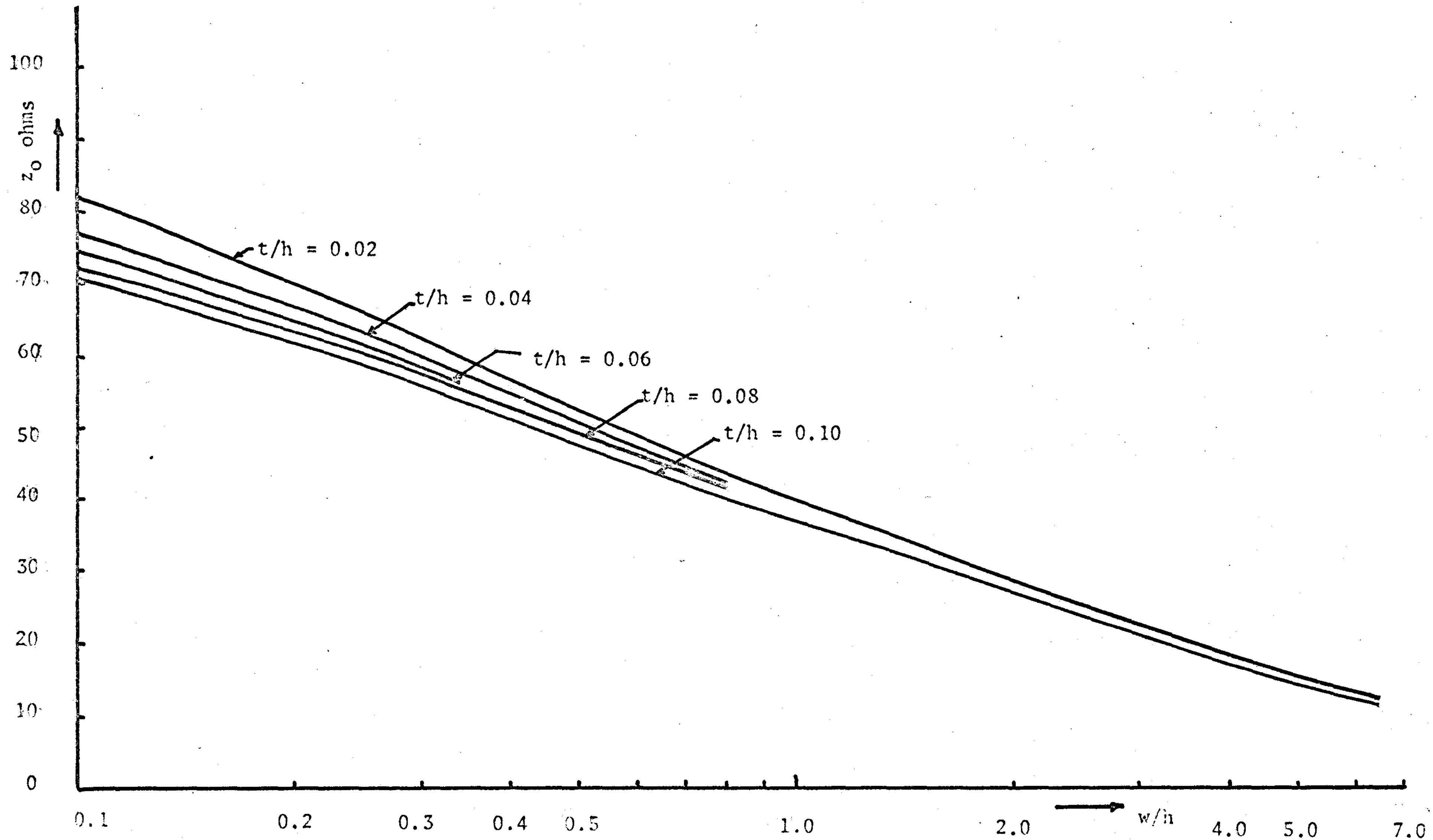

FIGURE 5.3(b): Characteristic Impedance of Microstrip Lines of Finite Strip Thickness on Germanium Substrates

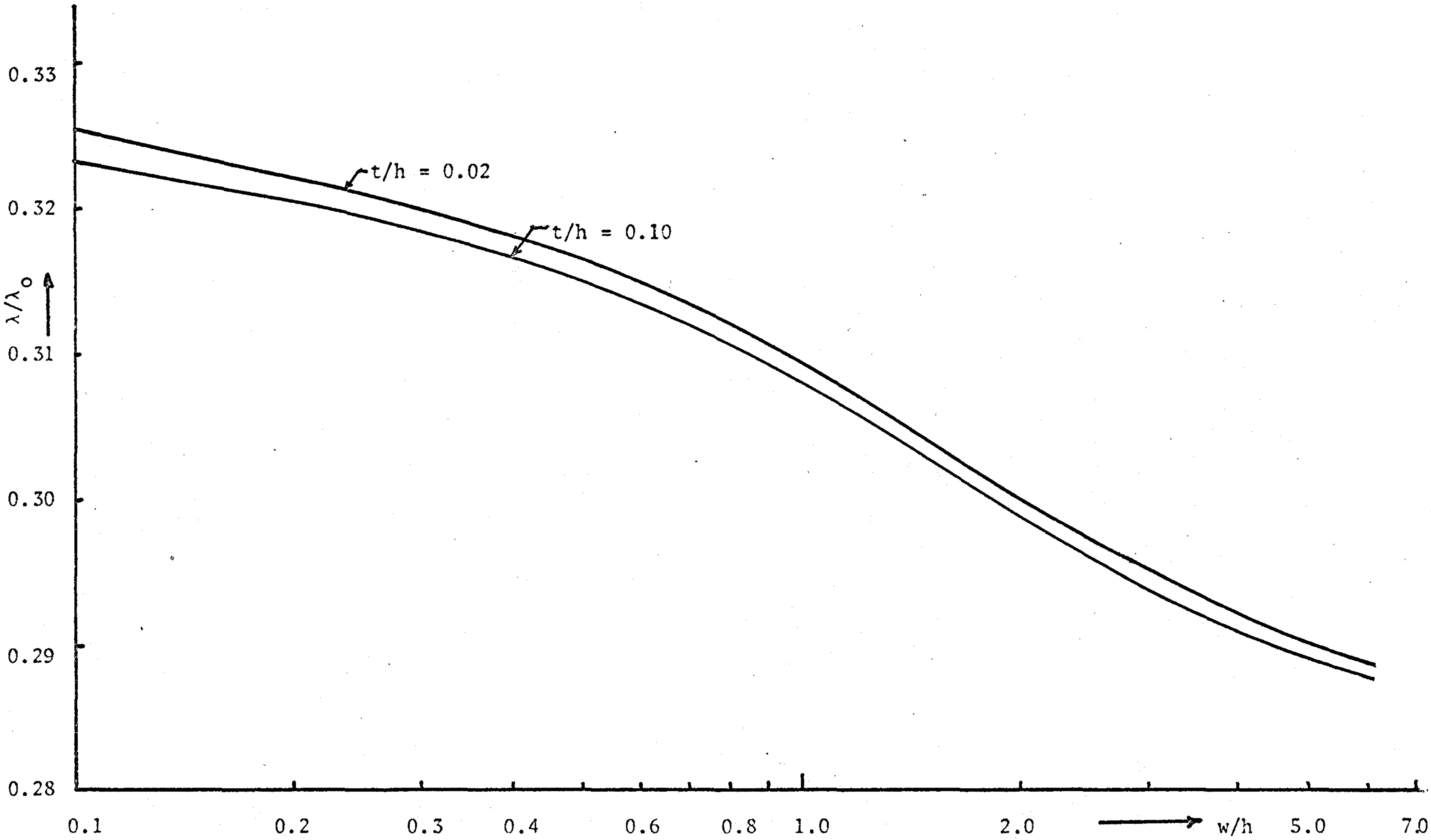

FIGURE 5.3(c): Guide Wavelength of Microstrip Lines of Finite Strip Thickness on Germanium Substrates

TABLE 5.3

Line Capacitance, Characteristic Impedance and Guide Wavelength of Two Dielectric Layer (ε_1 = 16.0, ε_2 = 7.0) Microstrips of Negligible Strip Thickness

	b/h = 1.004			b/h = 1.01			b/h = 1.02		
w/h	c/ε_o	z_o	λ/λ_o	c/ε_o	z_o	λ/λ_o	c/ε_o	z_o	λ/λ_o
0.1	12.70	88.52	.3353	11.93	91.33	.3459	11.07	94.81	.3591
0.4	19.69	59.25	.3231	19.01	60.30	.3288	18.09	61.812	.3371
0.7	24.93	47.71	.3170	24.25	48.37	.3214	23.27	49.37	.3281
1.0	29.71	40.61	.3124	29.01	41.10	.3162	27.96	41.86	.3221
1.3	34.30	35.60	.3087	33.55	35.99	.3121	32.43	36.61	.3175
1.6	38.77	31.82	.3056	37.97	32.15	.3988	36.76	32.68	.3139
1.9	43.13	28.85	.3030	42.28	29.13	.3061	40.99	29.59	.3109
2.2	47.40	26.43	.3009	46.51	26.69	.3038	45.12	27.09	.3084
2.5	51.59	24.44	.2991	50.64	24.66	.3018	49.18	25.03	.3063
2.8	55.70	22.75	.2975	54.71	22.95	.3002	53.16	23.28	.3046
3.1	59.75	21.30	.2963	58.70	21.49	.2989	57.08	21.79	.3031
3.4	63.73	20.04	.2952	62.64	20.21	.2977	60.94	20.49	.3019
3.7	67.68	18.93	.2943	66.54	19.08	.2968	64.76	19.35	.3008
4.0	71.60	17.94	.2935	70.42	18.09	.2960	68.56	18.33	.2999
4.3	75.53	17.05	.2929	74.29	17.19	.2953	72.35	17.41	.2992
4.6	79.49	16.23	.2923	78.20	16.36	.2947	76.19	16.57	.2986
4.9	83.53	15.47	.2918	82.19	15.59	.2942	80.09	15.80	.2980
5.2	87.72	14.75	.2914	86.34	14.87	.2937	94.15	15.06	.2975
5.5	92.20	14.06	.2909	90.75	14.17	.2932	88.46	14.35	.2970
5.8	97.16	13.37	.2903	95.63	13.47	.2926	93.21	13.65	.2964
6.1	103.2	12.64	.2984	101.4	12.75	.2918	98.81	12.91	.2955
7.4	148.05	9.10	.2799	145.8	9.17	.2820	142.2	9.28	.2855
8.7	184.3	7.48	.2737	181.5	7.53	.2758	177.1	7.63	.2792
10.0	200.86	6.95	.2702	197.9	7.00	.2723	191.13	7.08	.2756

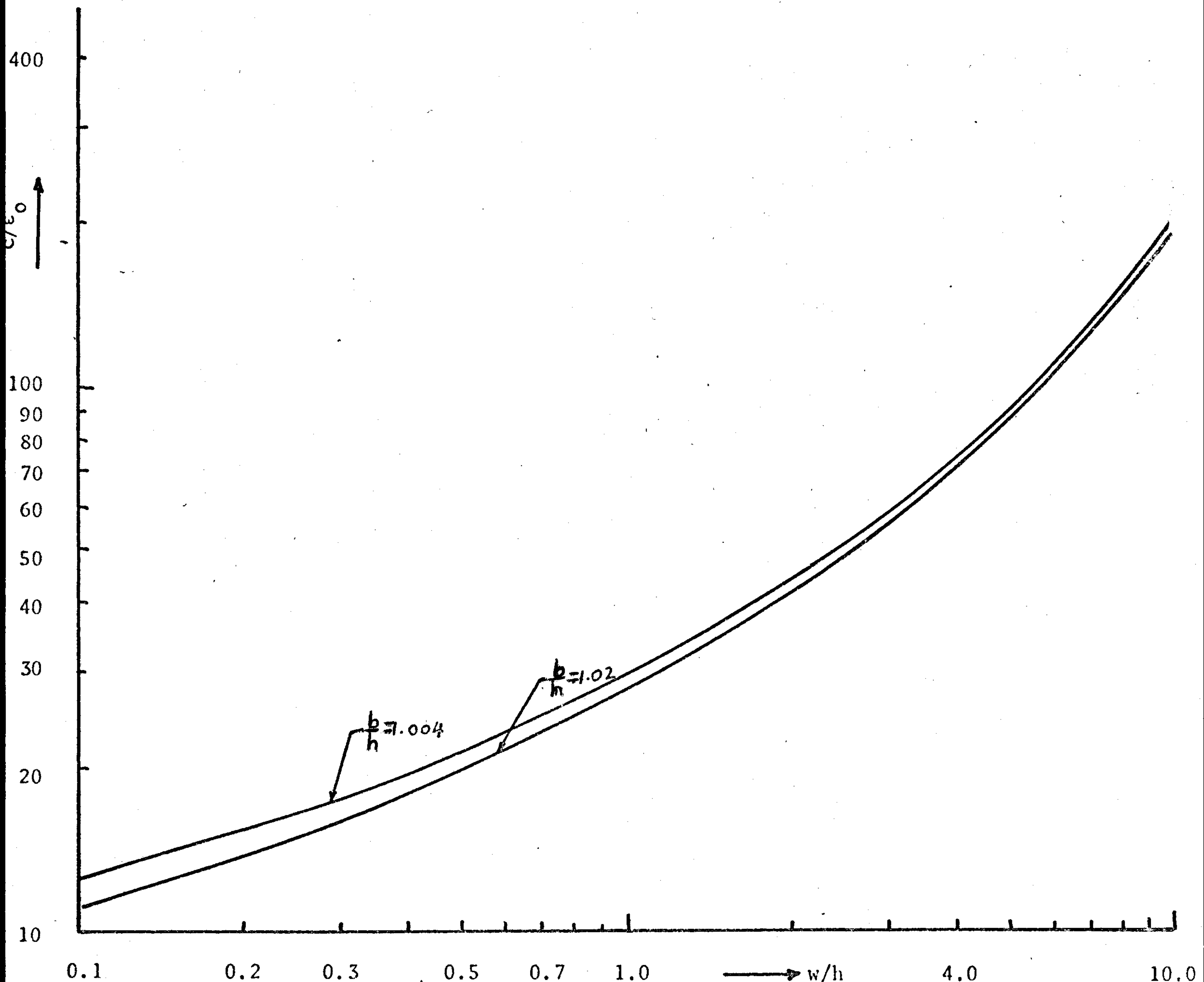

FIGURE 5.4(a): Line Capacitance of Two Layer Dielectric (ε_1 = 16.0, ε_2 = 7.0) Microstrip Lines of Negligible Strip Thickness

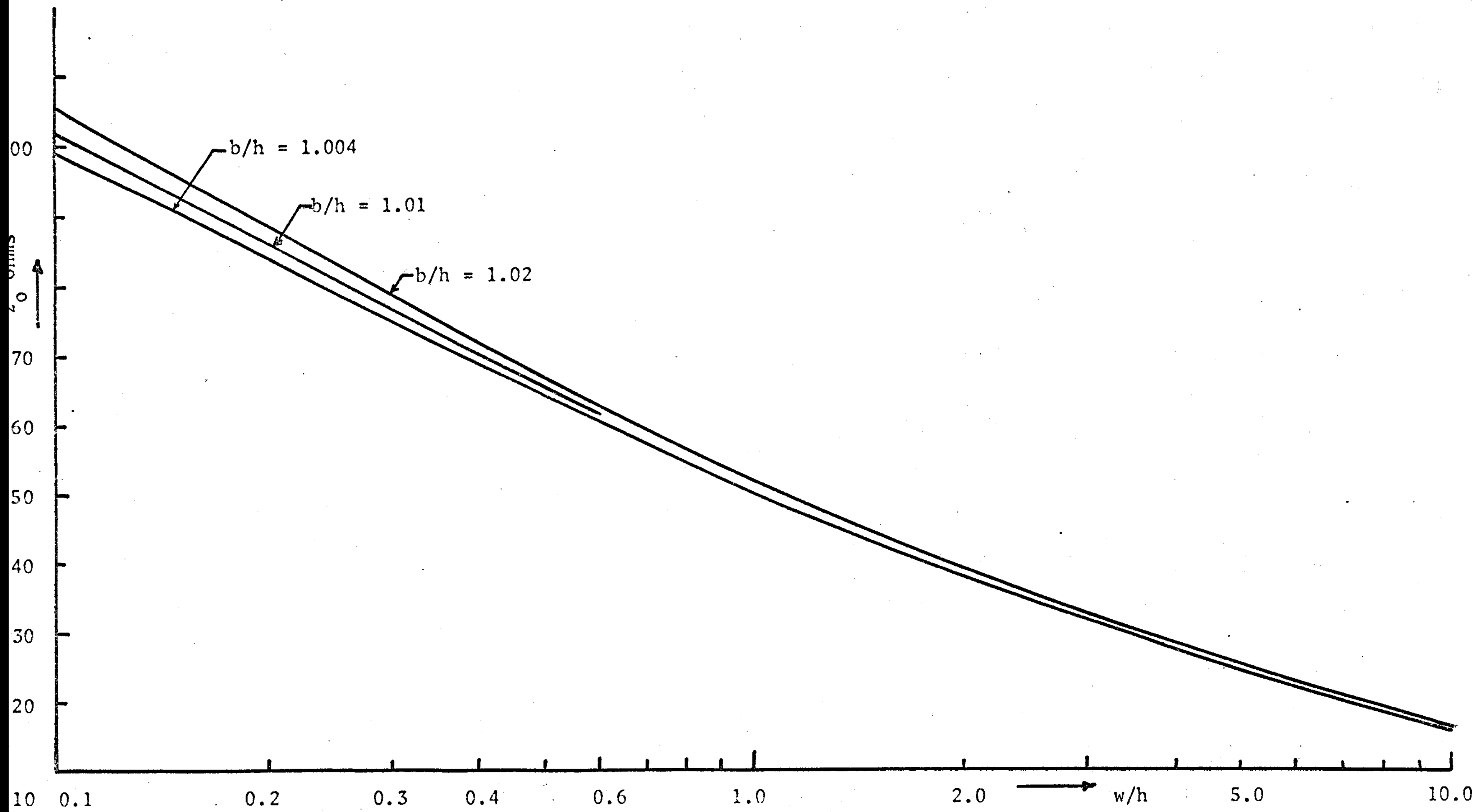

FIGURE 5.4(b): Characteristic Impedance of Two Dielectric Layer Microstrips (ε_1 = 16.0, ε_2 = 7.0) of Negligible Strip Thickness

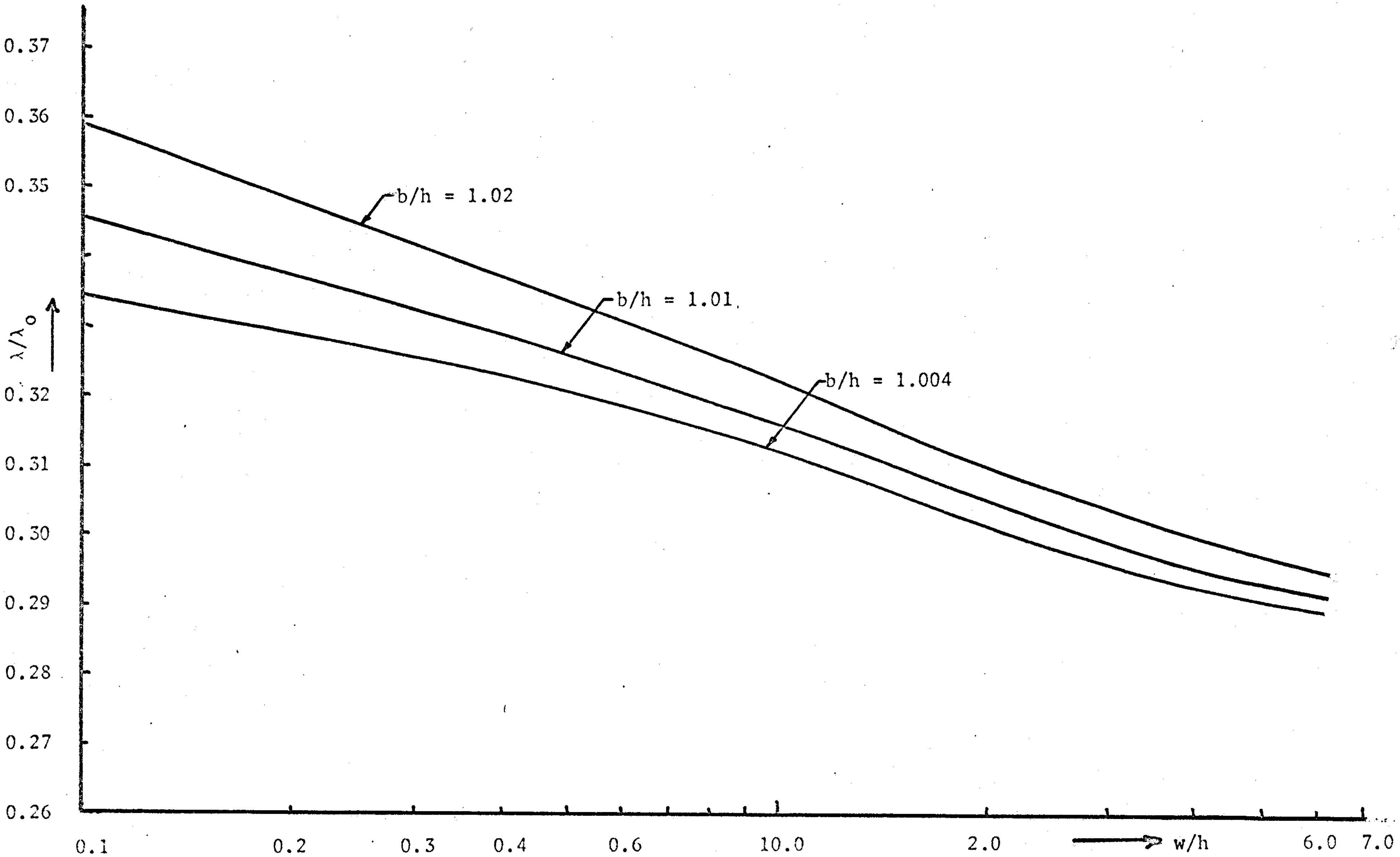

<u>FIGURE 5.4(c)</u>: Guide Wavelengths of Two Layer Dielectric ($\varepsilon_1 = 16.0$, $\varepsilon_2 = 7.0$) Microstrip Lines of Zero Strip Thickness

TABLE 5.4

Line Capacitance, Characteristic Impedance and Guide Wavelength of Two Dielectric Layer (ε_1 = 16.0, ε_2 = 7.0) Microstrips of Finite Strip Thickness (t/h = 0.05)

w/h	b/h = 1.004			b/h = 1.01			b/h = 1.02		
	c/ε_o	z_o	λ/λ_o	c/ε_o	z_o	λ/λ_o	c/ε_o	z_o	λ/λ_o
0.1	14.58	77.965	.3316	13.83	80.05	.3405	12.93	82.81	.3522
0.4	21.15	55.48	.3213	20.50	56.35	.3264	19.59	57.64	.3339
0.7	26.28	45.44	.3157	25.63	46.02	.3197	24.66	46.91	.3259
1.0	31.04	39.02	.3113	30.35	39.46	.3148	29.31	40.15	.3204
1.3	35.62	34.39	.3077	34.89	34.75	.3110	33.76	35.33	.3161
1.6	40.10	30.86	.3047	39.31	31.16	.3077	38.10	31.66	.3126
1.9	44.48	28.05	.3022	43.64	28.32	.3051	42.34	28.75	.3097
2.2	48.77	25.76	.3001	47.88	26.00	.3029	46.49	26.38	.3073
2.5	52.98	23.85	.2983	52.04	24.07	.3010	50.57	24.42	.3053
2.8	57.12	22.24	.2968	56.12	22.43	.2994	54.47	22.75	.3036
3.1	61.19	20.85	.2955	60.14	21.03	.2981	58.51	21.32	.3022
3.4	65.20	19.63	.2945	64.11	19.80	.2970	62.39	20.07	.3010
3.7	69.17	18.56	.2936	68.03	18.72	.2961	66.24	18.97	.3000
4.0	73.13	17.60	.2929	71.94	17.75	.2953	70.07	17.98	.2992
4.3	77.08	16.74	.2922	75.84	16.87	.2946	73.89	17.09	.2985
4.6	81.07	15.94	.2917	79.79	16.07	.2940	77.76	16.28	.2978
4.9	85.16	15.20	.2912	83.82	15.32	.2935	81.70	15.52	.2973
5.2	89.41	14.50	.2908	88.01	14.62	.2930	85.80	14.80	.2968
5.5	93.95	13.83	.2903	92.49	13.93	.2926	90.17	14.11	.2963
5.8	99.00	13.15	.2896	97.46	13.25	.2920	95.02	13.42	.2957
6.1	105.00	12.43	.2888	103.3	12.53	.2911	100.7	12.69	.2948

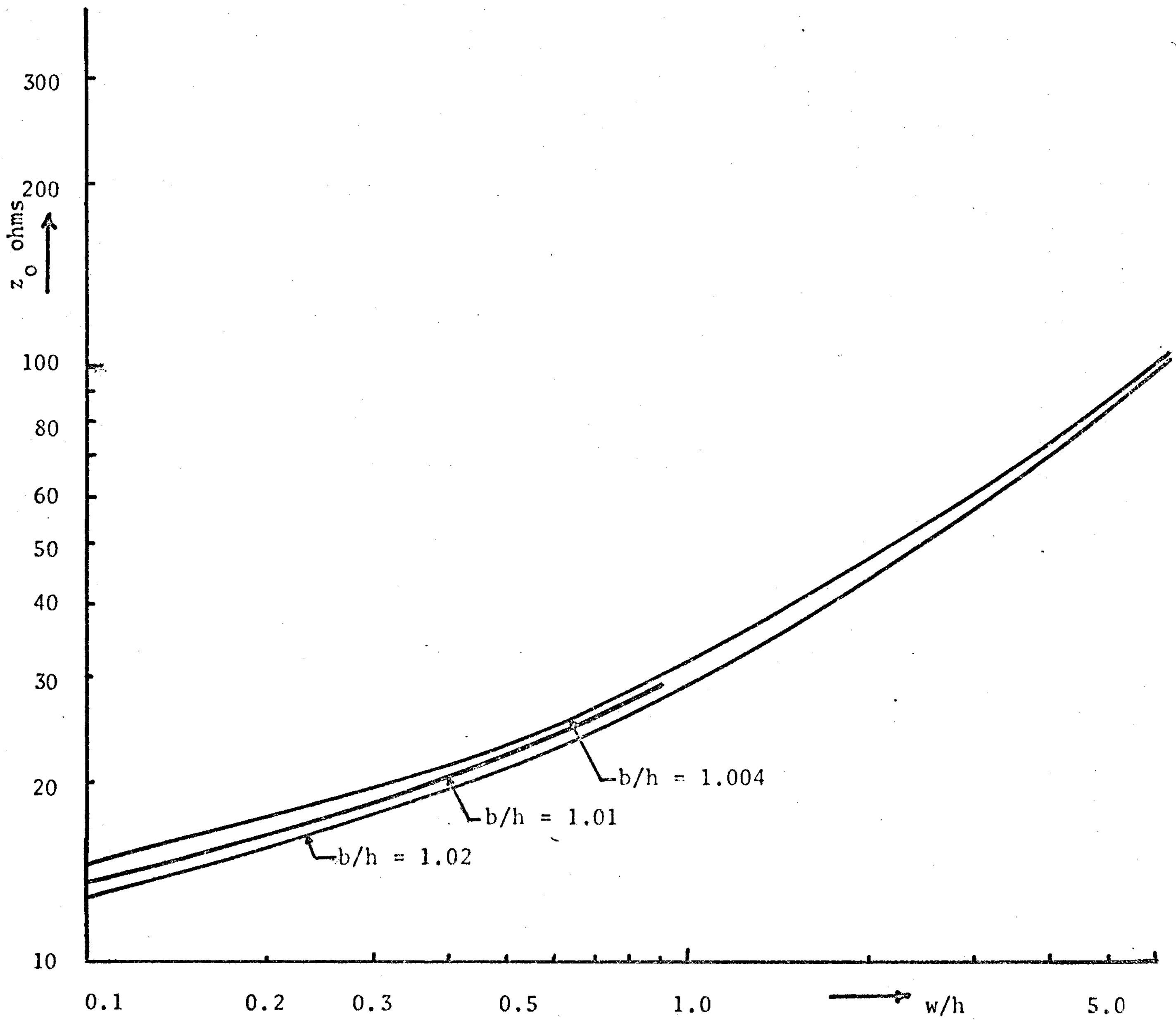

FIGURE 5.5(a): Capacitance of Two-Layer Dielectric (ε_1 = 16.0, ε_2 = 7.0) Microstrip Lines of Finite Strip Thickness (t/h = 0.05)

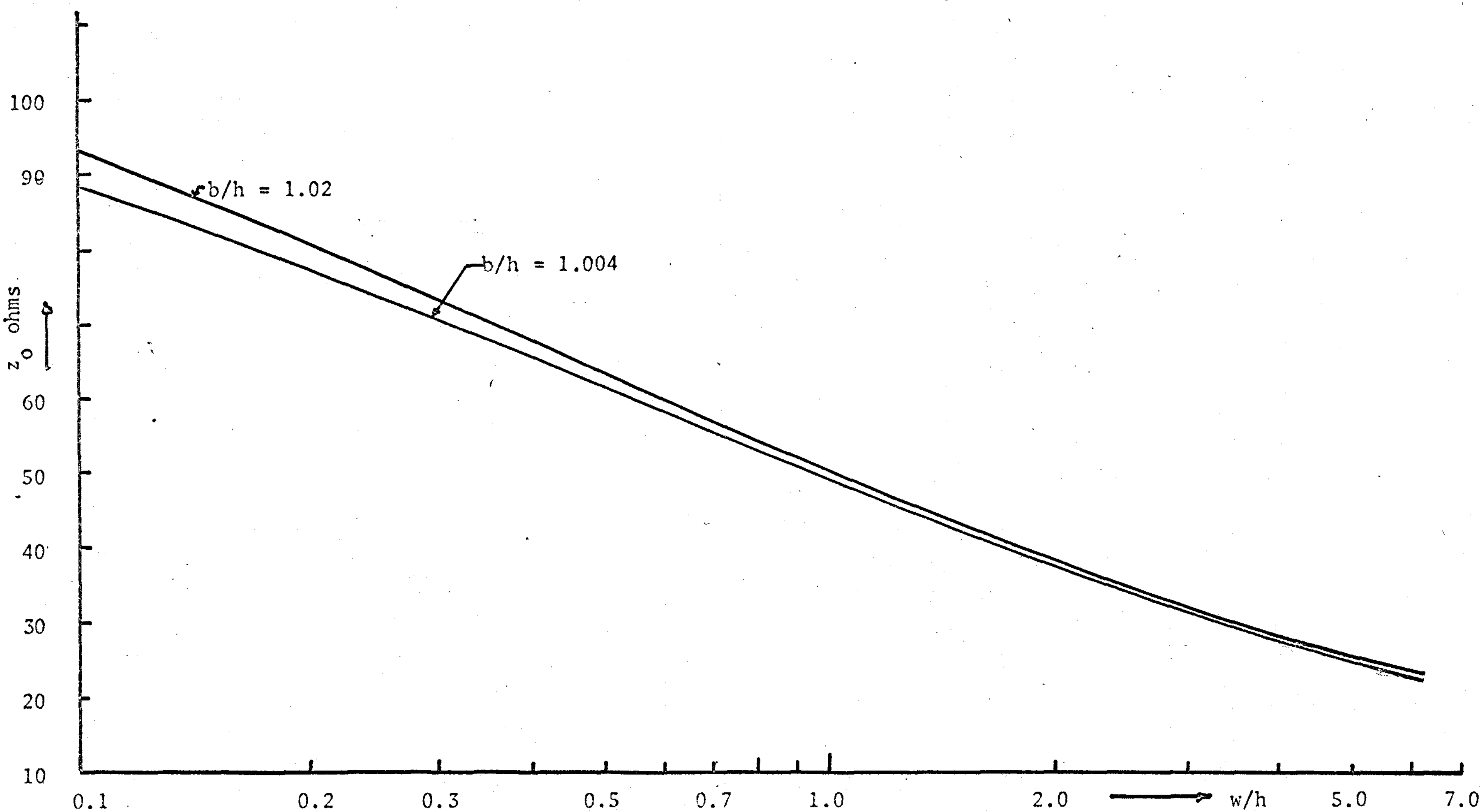

FIGURE 5.5(b): Characteristic Impedance of Two Dielectric Layer (ε_1 = 16.0, ε_2 = 7.0) Microstrips of Finite Strip Thickness (t/h = 0.05)

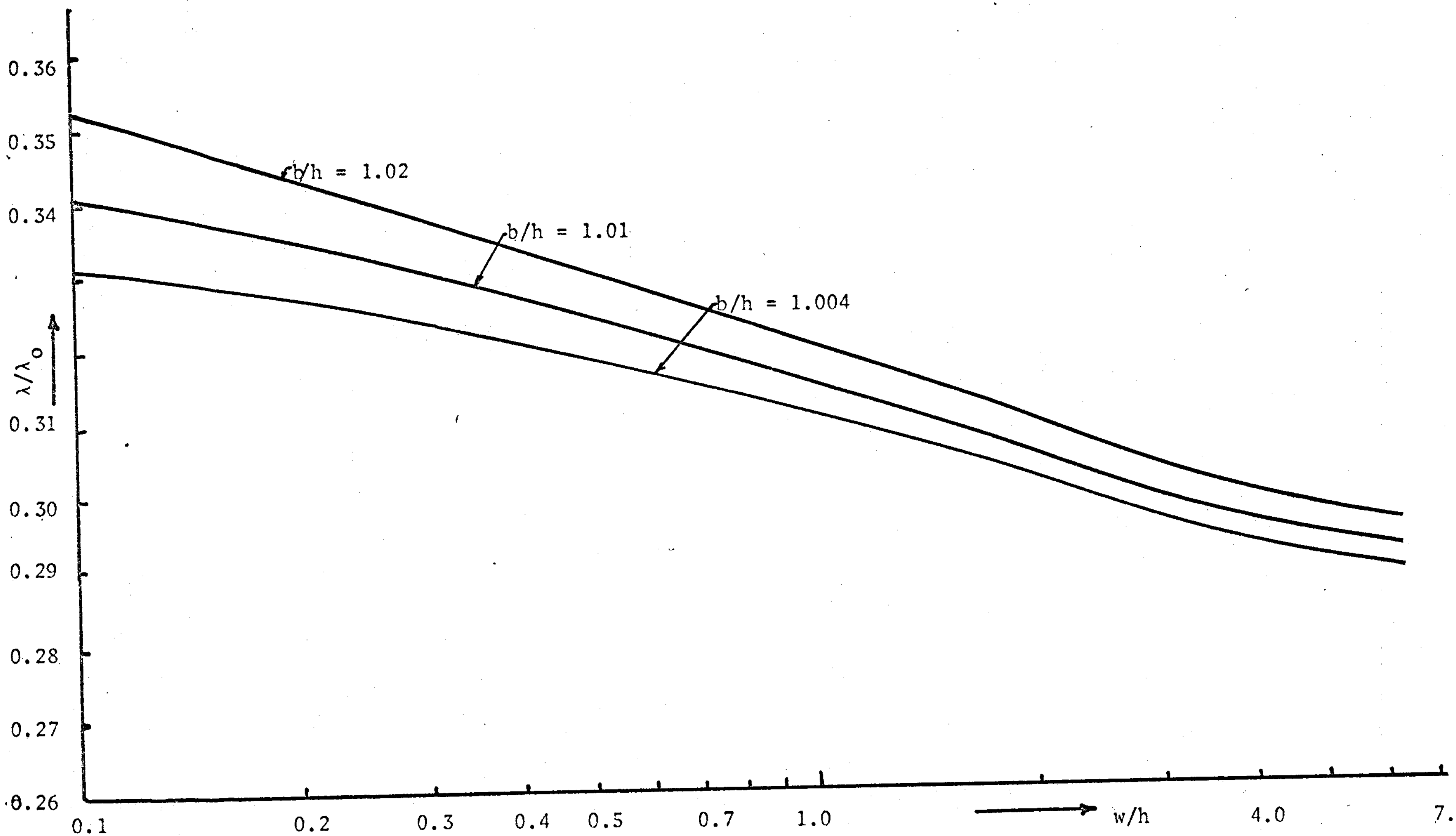

FIGURE 5.5(c): Guide Wavelength of Two Layer Dielectric (ε_1 = 16.0, ε_2 = 7.0) Microstrip Lines of Finite Strip Thickness (t/h = 0.05)

w mils	h mils	w/h	Z_o ohms	λg cm	Intrinsic Ge at 300°K $\rho \approx 47.2$ ohm-cm		Intrinsic Ge at 240°K $\rho \approx 2000$ ohm-cm	
					αdb/cm	αdb/λg	αdb/cm	αdb/λg
12.5	57	0.22	70	1.0298	1.416	1.458	0.0334	0.0344
20	35	0.57	51.5	1.0116	2.699	2.730	0.0637	0.0644
31	42	0.74	46.5	1.0036	3.164	3.175	0.0747	0.0749
64	40	1.60	33.0	0.9716	4.855	4.717	0.1146	0.1113
63	24	2.62	24.0	0.9467	5.782	5.474	0.1364	0.1292
137	27	5.07	15.0	0.9189	6.993	6.426	0.1650	0.1516

TABLE 5.5: Total Losses in Microstrip Transmission Lines On Intrinsic Germanium Substrates

5.2 EXPERIMENTAL RESULTS:

5.2.1 Measurement of the Scattering Parameters of the Waveguide-Microstrip Line Junction

The experimental readings for the precision attenuator (A) and the precision short (ℓ) at the points P_1, P_2, P_3 and P_4 of the 50 ohm microstrip line on air dielectric is given in Table 5.6. Also given are the magnitudes and phases of the reflection coefficients at these points:

$f = 9.38$ GHz
$A = 0.0$
$\ell = 0.655$ cm

Point	A db	ℓ(cm)	ρ	$\phi°$
P_4	0.28	0.225	0.936	249
P_3	0.14	1.875	0.970	-15
P_2	0.44	1.247	0.905	86
P_1	0.51	0.745	0.89	165.5

TABLE 5.6

The points P_1, P_2, P_3 and P_4 have been plotted on a polar graph in Figure 5.6, and by simple construction the scattering parameters of the junction have been found to be: -

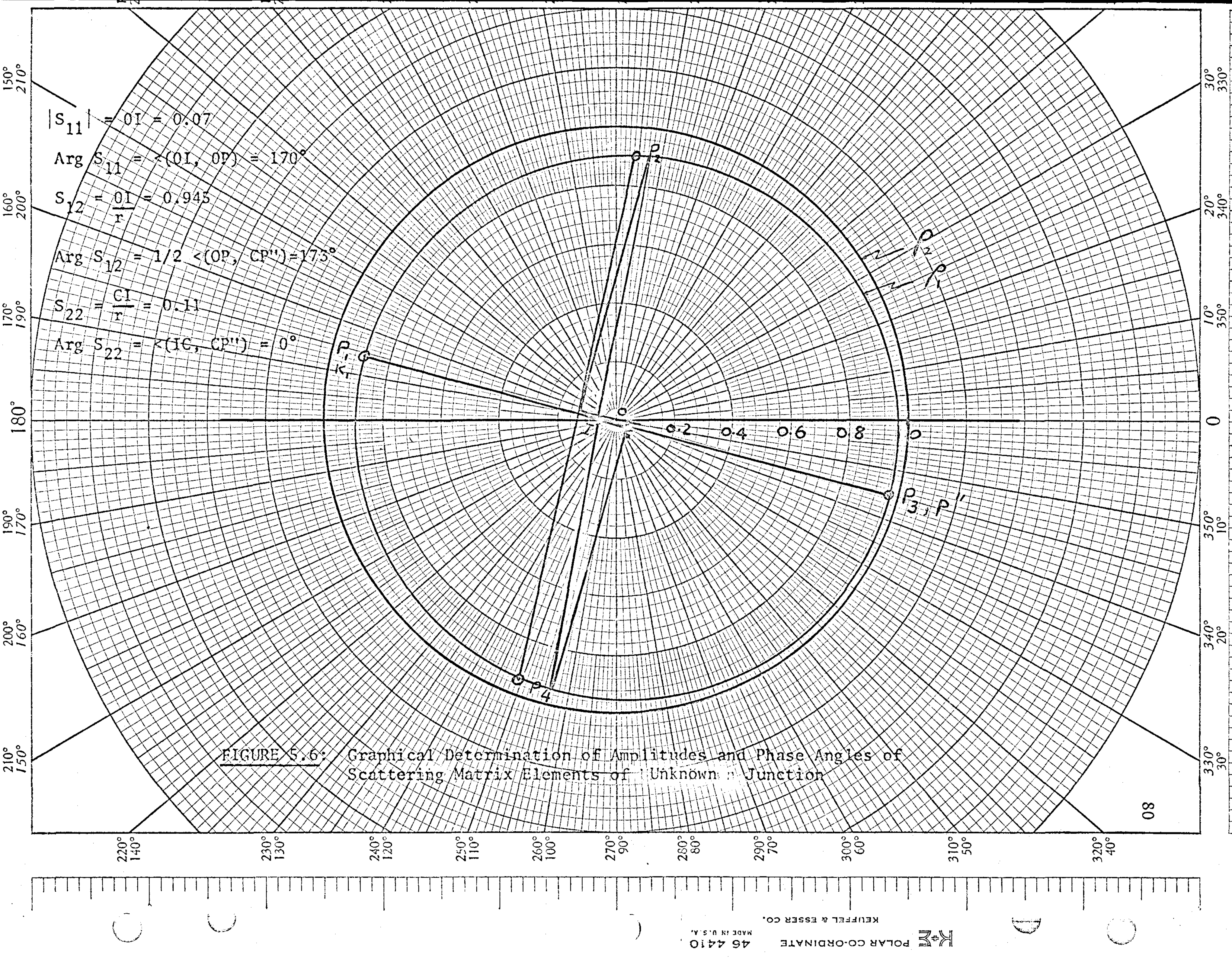

FIGURE 5.6: Graphical Determination of Amplitudes and Phase Angles of Scattering Matrix Elements of Unknown Junction

$$S_{11} = 0.07[\cos(2.958) + j \sin(2.958)]$$

$$S_{12} = 0.945[\cos(3.01) + j \sin(3.01)]$$

and $$S_{22} = 0.11 < 0°.$$

The efficiency of the waveguide to microstrip line junction will be equal to:

$$\eta = -20 \log_{10}|S_{12}| \text{db}$$

$$= 20 \log 1.0582$$

$$= 0.48 \text{ db}$$

5.2.2 Dimensions of the Samples

The dimensions of the microstrip lines on intrinsic germanium substrates have been measured as described in Chapter IV and are given in Table 5.7.

w mils	h mils	w/h
12.5 ± 0.1	57 ± 1	0.22 ± 0.004
20 ± 0.1	35 ± 1	0.57 ± 0.01
31 ± 0.1	42 ± 1	0.74 ± 0.02
64 ± 0.1	40 ± 2	1.6 ± 0.1
63 ± 0.1	24 ± 1	2.6 ± 0.1
137 ± 0.1	27 ± 0.5	5.1 ± 0.05

TABLE 5.7

Measurement of the Characteristic Impedances of the Microstrip Lines

Given in Table 5.8 are the measured short circuit, open circuit and characteristic impedances of the experimental microstrip lines. A comparison between the measured and the theoretical values is made in Figure 5.9:

$$f = 9.380 \text{ GHz}$$

$$A_o = 0 \quad , \quad \ell_o = 0.705 \text{ cm.}$$

w/h	A	ℓ	$z_{O.C.}$	$z_{S.C.}$	$Z_o = 50\sqrt{z_{O.C.} z_{S.C.}}$ ohms
0.22	8.86 5.38	1.70 1.325	1.4812	1.12	64.5
0.57	3.73 3.84	1.185 1.178	0.7505	0.7448	52
0.714	7.79 3.10	1.415 1.320	12437	1.0933	46.6
1.6	3.84 4.26	1.110 1.0850	0.69593	0.6879	34
2.62	5.38 3.22	0.700 0.785	0.6161	0.3563	22
5.07	2.07 3.22	0.955 0.965	0.34035	0.4543	19.6

TABLE 5.8

Experimental Results

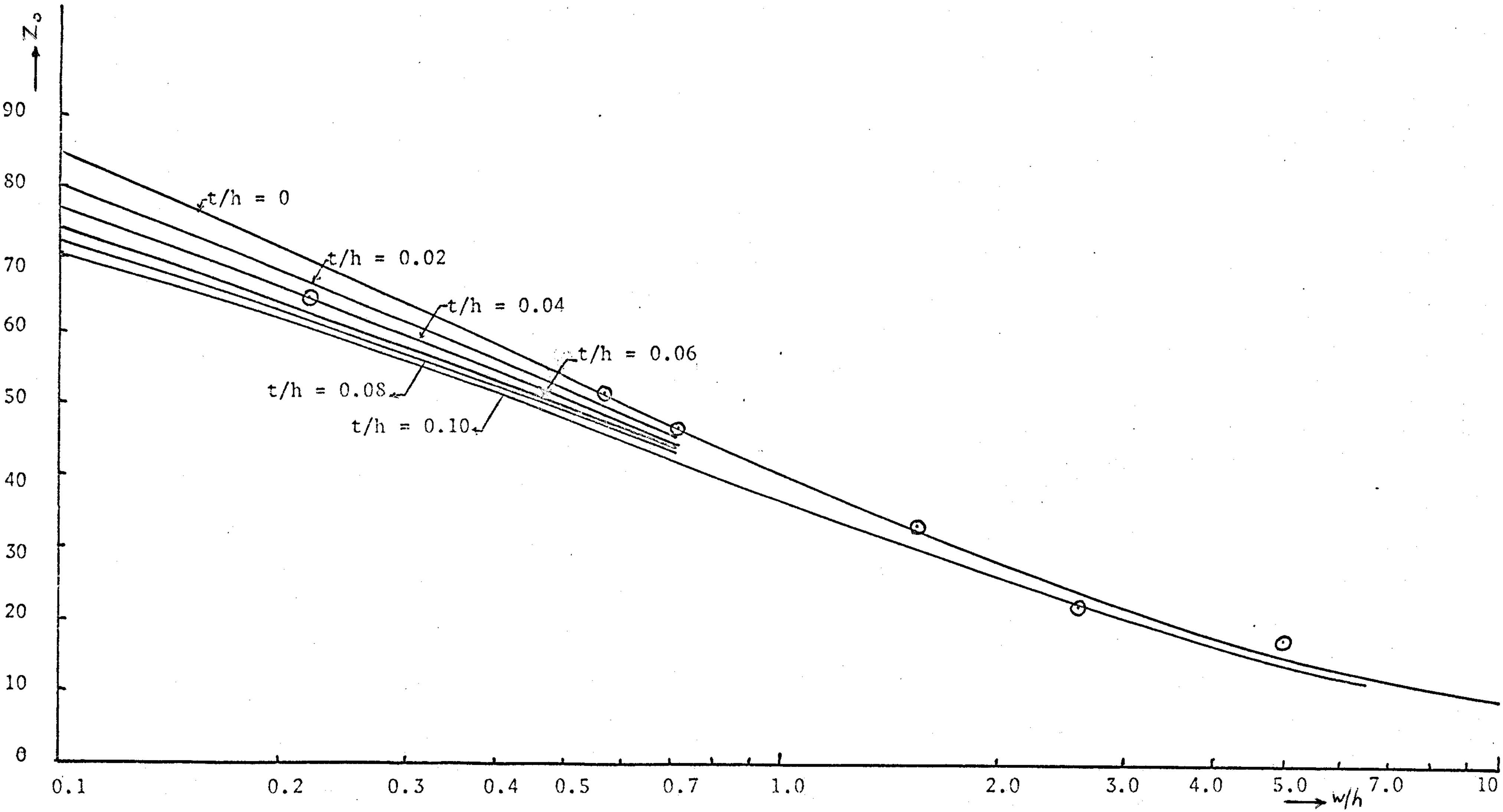

FIGURE 5.7: Comparison Between Experimental and Theoretical Values of the Characteristic Impedance of Microstrip Lines on Intrinsic Ge substrates

CHAPTER VI

CONCLUSIONS

The transmission properties of microstrip lines for microwave I.C.'s have first been analysed by applying a suitable Schwarz-Christoffel transformation to a parallel plate structure of negligible plate thickness. Two transcendental equations were obtained and were numerically solved using the Newton-Raphson method. Subsequently, by a simple analogy, the characteristic impedance of the microstrip structure has been calculated as a function of line dimensions for the case of germanium substrates ($\varepsilon_r = 16.0$). This approximate solution is compared to Wheeler's solution in Figure 5.1, and it is seen that a good agreement (to within ± 2 ohms) has been obtained for values of $\frac{w}{h} \geq 0.6$. For values of $\frac{w}{h} \lesssim 0.6$, the original assumption that the plates are wide is no longer valid, giving inaccurate results.

This analysis, which has been based on a TEM propagation, neglects the dielectric discontinuity at the substrate boundary, and is unable to account for a finite conductor thickness. However, despite its shortcomings, this method has provided useful design equations (equations 2.15 and 2.16) for values of characteristic impedances $\lesssim 50$ ohms when using substrates having $\varepsilon_r \lesssim 16.0$ (see Figure 5.1)

It is interesting to note that for large values of $\frac{w}{h}$, an approximate expression for the characteristic impedance has been derived (equation 2.17) which is identical to that obtained by Assadourian and Rimai[12] in 1952 using a different mapping function.

A second method which has been used to analyse microstrip structures is based on the application of Fourier transform and variational techniques to compute the line capacitance, characteristic impedance and guide wavelength of the structure as a function of line dimensions and substrate dielectric constant. The following microstrip structures have been considered:

(a) Microstrip transmission lines on single layer dielectric substrates having negligible and finite strip conductor thickness.

(b) Microstrip transmission lines on double layer dielectric substrates having negligible and finite strip conductor thickness.

It should be mentioned that the author derived all the expressions in case (b) independently of E. Yamashita[30].

As mentioned in Chapter I, microwave I.C's (both hybrid and monolithic) are now being extensively used in the design and implementation of microwave circuits. At high frequencies microstrip on semiconductor substrates (especially silicon) is of interest so that the microwave circuits may be constructed on the same material as the active device. Applications involving relatively high power require that the active devices be passivated in order that sufficiently high breakdown voltages be maintained. At present these passivation techniques include the use of grown or deposited silicon dioxide films and/or Al_2O_3 films. Silicon nitride is still being investigated as a passivating element.

It is because of the above reasons that the analysis of multilayer dielectric microstrip structures is so important. Design charts have been provided for the case of intrinsic germanium substrates in case (a) above (shown from Figure 5.2(a) to Figure 5.3(c)) and intrinsic germanium coated with a thin film of Al_2O_3 ($\varepsilon_r \approx 7.0$) in case (b) (shown from Figure 5.4(a) to Figure 5.5(c)). To show the effect of a thin film of Al_2O_3 on the propagation characteristics of a microstrip transmission line, the following two cases will be considered: -

(i) $\frac{w}{h} = 0.1$, $t/h = 0.05$, $b/h = 1.01$

$\therefore Z_o = 80\Omega$, $\frac{\lambda}{\lambda_o} = 0.3405$

(ii) $\frac{w}{h} = 0.1$, $t/h = 0.05$, $b/h = 1.00$

$\therefore Z_o = 75.6\Omega$, $\frac{\lambda}{\lambda_o} = 0.3244$

Therefore the characteristic impedance will increase by approximately 4.4Ω (5.8%) by the addition of a thin (0.01 h) passivating layer of Al_2O_3. This increase is Z_o with oxide layer present will tend to get smaller for larger values of $\frac{w}{h}$.

The variational method can be extended to analyse multilayer dielectric microstrip structures since it is possible to take into account all dielectric boundary conditions no matter how many planar boundaries exist in these lines. The line capacitance characteristic impedance and guide wavelength of such structures can be obtained for a wide range of structural parameters, and the thickness of the strip can also be taken into account.

The approximate losses incurred in microstrip lines on semiconductor substrates have been calculated (or analyzed). This analysis was based on the assumption of a constant current distribution on the strip conductor to facilitate the analysis. The approximate losses in some particular microstrip lines on intrinsic germanium substrates have thus been calculated at room temperature ($\rho \cong 47.4$ ohm-cm) and at 240°K ($\rho \cong 2000$ ohm-cm) to show that high resistivity semiconductors have small dielectric losses. Thus for w = 12.5 mils, h = 57 mils, w/h = 0.22 and at 300°K α = 1.416 db/cm while at 240°K α = 0.0334 db/cm. Another way of expressing the dielectric loss is through the dissipation factor D which is given by:

$$D = \frac{1}{\omega RC}$$

Substituting $R = \frac{\rho \ell}{A}$, and $C = \frac{\varepsilon A}{\ell}$ gives:

$$D = \frac{1}{\omega \rho \varepsilon}$$

at f = 9.38 GHz, $\varepsilon = 16 \times \frac{1}{36\pi} \times 10^{-9}$ and ρ = 47.4 ohm-cm, D = 0.253. The quality factor of the dielectric Q_d is given by:

$$Q_d = \omega \varepsilon \rho = 3.95$$

To obtain a small dielectric loss (which is predominant in monolithic microwave I.C's), a semiconductor substrate should have D << 1 (or Q_d >> 1) and therefore have a high resistivity at room temperature. Thus silicon and gallium arsenide make much better semiconductor substrates for monolithic microwave I.C's. However, for intrinsic germanium at 240°K, D = 0.006, and Q_d = 166.7 resulting in a small overall loss.

It therefore follows that intrinsic germanium is not a good substrate for microstrip structures at room temperature.

An experimental technique (based on the Deschamps method) for measuring the characteristic impedance of microstrip lines has been described in detail. This method makes use of a high precision reflection bridge similar to that suggested by Champlin et al[26] which gives the magnitude and phase of the reflection coefficient at the input plane of the waveguide to microstrip transition.

The scattering parameters of the lossy waveguide to microstrip function have been experimentally determined in magnitude and phase as described in Chapter IV. The experiment has been carefully repeated more than twenty times until good accuracy was ensured (to within ± 5%, it is believed).

Six microstrip lines having different line dimensions have been carefully built on thin intrinsic germanium wafers using an Edwards high vacuum unit. The characteristic impedances of the lines have been measured at 9.38 GHz and compared with the theoretical values as calculated by the variational technique (shown in Figure 5.7). Since it is estimated that $t \cong 3.00$ microns, and the smallest value of $h = 24$ mils, therefore $t/h < 0.005$. Hence a good agreement between the theoretical and practical results has been obtained. However, it must also be concluded that because of its inherently high dissipation factor, intrinsic germanium is unsuitable for use as a substrate in practical monolithic microwave integrated circuits.

APPENDIX I

C O M P U T E R   P R O G R A M M E S

```
$JOB    WATFOR  003531 DIMYAN              100    010    030
$IBJOB          NODECK
$IBFTC
C       ANALYSIS OF MICROSTRIP LINES BY MEANS OF VARIATIONAL MEATHODS
C        USING SIMPSONS RULE
        PI=3.1416
40        READ (5,12) EPSI
12      FORMAT (F13.4)
         AG=0.166666667/(EPSI*PI)
        AG0=0.16666667/PI
          R=0.1
50       X=0.5
        SUM=0.0
         AS=0.00
20       A=2.*(SIN(X*R/2.))/(X*R/2.)
         B=(SIN(X*R/4.))/(X*R/4.)
          C=EPSI+TANH(X)
        AC=1.0+TANH(X)
         Y=(TANH(X)*((A-B**2)**2))/(C*X*PI)
         AY=(TANH(X)*((A-B**2)**2))/(AC*X*PI)
       SUM1=SUM+Y
       SUM=SUM1
         Z=0.66666667*SUM
        AS1=AS+AY
        AS=AS1
           AZ=0.666666667*AS
14         X=X+1.0
         IF (X.LT.79.5) GO TO 20
        IF (X.EQ.79.5) GO TO 45
45       Z1=Z
         AZ1=AZ
         X0=1.0
        S0=0.0
          AS0=0.0
30        A0=2.*(SIN(X0*R/2.))/(X0*R/2.)
       B0=(SIN(X0*R/4.))/(X0*R/4.)
          C0=EPSI+TANH(X0)
         AC0=1.0+TANH(X0)
        Y0=(TANH(X0)*(A0-B0**2)**2)/(C0*X0*PI)
         AY0=(TANH(X0)*(A0-B0**2)**2)/(AC0*X0*PI)
        S=S0+Y0
       S0=S
         Z0=0.333333333*S0
         AS2=AS0+AY0
              AS0=AS2
         AZ0=0.333333*AS0
15         X0=X0+1.0
        IF (X0.LT.80.) GO TO 30
         IF (X0.EQ.80.) GO TO 55
55        Z2=Z0
          AZ2=AZ0
         C1=1.0/(AG+Z1+Z2)
         C2=1.0/(AG0+AZ1+AZ2)
         CI=120.*PI/SQRT(C1*C2)
         AL=SQRT(C2/C1)
         WRITE(6,70) EPSI,R,C1,C2,CI,AL
70        FORMAT(1P6E16.4)
         R=R+0.3
```

```
       IF (R.LE.6.1) GO TO 50
       R=R+1.0
        IF (R.LE.10.1) GO TO 50
       IF (EPSI.LE.16.) GO TO 40
      STOP
      END
$ENTRY
11.7
16.0
$IBSYS
```

```
$JOB    WATFOR  003531 DIMYAN              100   010   030
$IBJOB          NODECK
$IBFTC
C          ANALYSIS OF MICROSTRIP LINES OF FINITE CONDUCTOR THICKNESS
C         HAVING TWO DIELECTRIC LAYERS USING THE VARIATIONAL METHOD
       PI=3.14159
40      READ (5,12) Y
12      FORMAT (F13.3)
        EPSI1=16.00
       EPSI2=7.0
        R=EPSI2-EPSI1
         S=EPSI1+EPSI2
        T=EPSI2-1.
         P=EPSI2+1.
        G=(2.*Y/(P+T)+4.*R/((P+T)*(S-R)))/PI
        AG=0.166666667*G
        AG0=0.1666667/PI
        F=0.1
50       X=0.5
         S1=0.05
       SUM=0.0
        AS=0.00
20      A=2.*(SIN(X*F/2.))/(X*F/2.)
        B=(SIN(X*F/4.))/(X*F/4.)
       RE=R*EXP(-2.0*(Y-1.)*X)
       SE=S*EXP(-2.0*X*Y)
       RA=R*EXP(-2.0*X)
       SA=S*EXP(-2.0*(1.-Y)*X)
       RB=R*EXP(-2.0*(2.-Y)*X)
       SB=S*EXP(-2.0*X)
       C=1.0/(P-((RE-SE)*T)/(S-RA))
       D=(R-SB)/((SA-RB)*P-T*(R-SB))
        U=0.5*(1.+EXP(-X*S1))*((A-B**2)**2)*(C+D)/(X*PI)
        AC=1.0+TANH(X)
        AU=0.5*(1.+EXP(-X*S1))*(TANH(X)*(A-B**2)**2)/(AC*X*PI)
        SUM1=SUM+U
        SUM=SUM1
26       Z=0.66666667*SUM
       AS1=AS+AU
        AS=AS1
        AZ=0.6666667*AS
       X=X+1.0
        IF (X.LT.99.5) GO TO 20
        IF (X.EQ.99.5) GO TO 45
45      Z1=Z
        AZ1=AZ
        X0=1.0
       S0=0.0
       AS0=0.0
30       A0=2.*(SIN(X0*F/2.))/(X0*F/2.)
        B0=(SIN(X0*F/4.))/(X0*F/4.)
       RE0=R*EXP(-2.0*(Y-1.)*X0)
       SE0=S*EXP(-2.0*X0*Y)
       RA0=R*EXP(-2.0*X0)
       SA0=S*EXP(-2.0*(1.-Y)*X0)
       RB0=R*EXP(-2.*(2.-Y)*X0)
        SB0=S*EXP(-2.0*X0)
       C0=1.0/(P-((RE0-SE0)*T)/(S-RA0))
```

```
      D0=(R-SB0)/((SA0-RB0)*P-T*(R-SB0))
      U0=0.5*(1.+EXP(-X0*S1))*((A0-B0**2)**2)*(C0+D0)/(X0*PI)
      AC0=1.0+TANH(X0)
      AU0=0.5*(1.+EXP(-X0*S1))*(TANH(X0)*(A0-B0**2)**2)/(AC0*X0*PI)
      S2=S0+U0
       S0=S2
27      Z0=0.33333333*S0
      AS2=AS0+AU0
      AS0=AS2
      AZ0=0.33333333*AS0
     X0=X0+1.0
      IF (X0.LT.100.0) GO TO 30
      IF (X0.EQ.100.0) GO TO 55
55    Z2=Z0
      AZ2=AZ0
      C1=1.0/(AG+Z1+Z2)
      C2=1.0/(AG0+AZ1+AZ2)
      CI=120.*PI/SQRT(C1*C2)
      AL=SQRT(C2/C1)
      WRITE(6,70) Y,F,C1,C2,CI,AL
70     FORMAT(1P6E14.4)
     F=F+0.3
     IF (F.LE.6.1) GO TO 50
78     F=F+1.0
      IF (F.LE.10.1) GO TO 50
     IF (Y.LE.1.1) GO TO 40
     STOP
      END
$ENTRY
1.004
1.01
1.02
$IBSYS
```

16905

```
$JOB    WATFOR  003531 DIMYAN              100    010    030
$IBJOB          NODECK
$IBFTC
C          EXPERIMENTAL DETERMINATION OF MICROSTRIP IMPEDANCE
C          USING THE DESCHAMPS METHOD
         REAL F,B,AL1,AL2, A,D,T0,T1,A0,A1,G,PHI,ABSVAL,PHASE,Y,EPSI
          COMPLEX S11,S22,S12,RHO1,RHO,Z0 ,Z
          F=9.38E+9
          A=2.3
          AL1=3.E+10/F
           D=(1.-(AL1/(2.*A))**2)**0.5
         AL2=AL1/D
           B=2.*3.1416/AL2
         S11=CMPLX(0.07*COS(2.958),0.07*SIN(2.958))
         S12=CMPLX(0.945*COS(3.01),0.945*SIN(3.01))
         S22=CMPLX(0.11*COS(0.0),0.11*SIN(0.0))
          A0=0.0
          T0=0.705
 5        READ (5,30) A1,T1
30        FORMAT(2F10.0)
         G=EXP(2.*(A0-A1)/8.69)
          PHI=2.*B*(T0-T1)+3.1416
         RHO1=CMPLX(G*COS(PHI),G*SIN(PHI))
         Z=(1.+RHO1)/(1.-RHO1)
         Y=CABS(Z)
         EPSI=57.296*ATAN2(AIMAG(Z),REAL(Z))
         RHO=(RHO1-S11)/(S12**2+S22*(RHO1-S11))
          Z0=(1.+RHO)/(1.-RHO)
           ABSVAL=CABS(Z0)
         PHASE=57.296*ATAN2(AIMAG(Z0),REAL(Z0))
          WRITE(6,40)A1,T1,Y,EPSI,ABSVAL,PHASE
40       FORMAT(1P6E14.4)
          IF (A1.LT.15.) GO TO 5
          STOP
          END
$ENTRY
8.86       1.700
5.38       1.325
3.73       1.185
3.84       1.178
7.79       1.415
3.84       1.110
3.10       1.320
4.26       1.085
5.38       0.6500
3.22       0.7800
2.07       0.955
3.22       0.965
$IBSYS

                                      CD TOT    0049
```

APPENDIX II

PHOTOGRAPHS

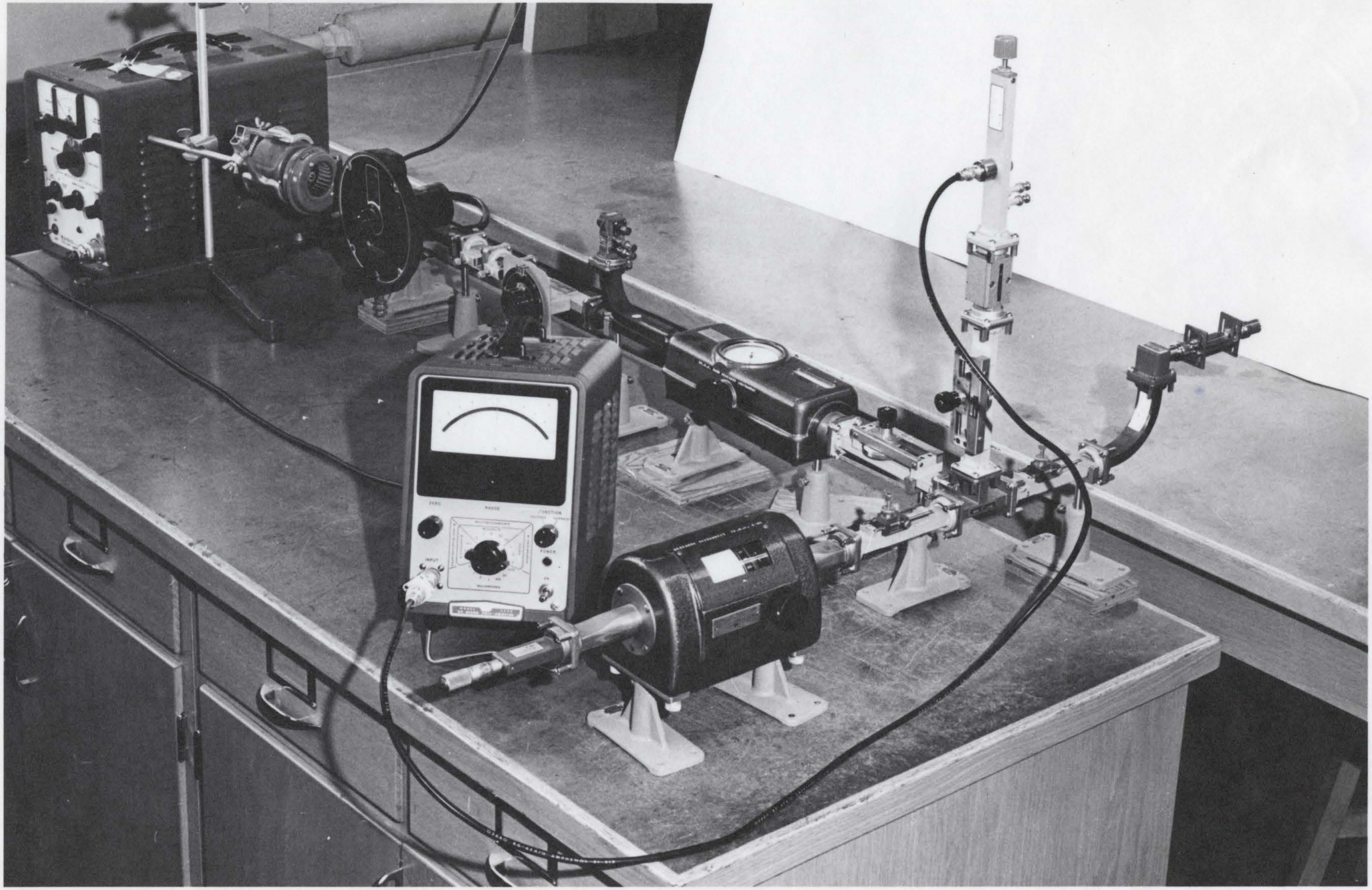

PHOTOGRAPH I: The Experimental Setup of the Microwave Bridge

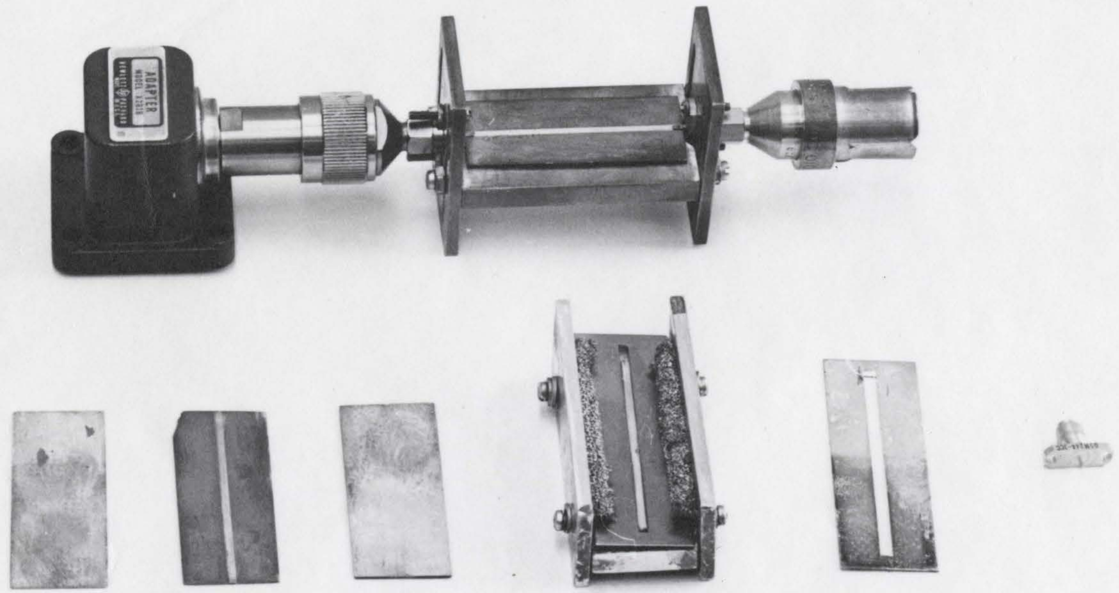

(a)

(b) (c) (d) (e)

PHOTOGRAPH II: (a) Microstrip Jig, (b) top and bottom view of the Microstrip Line, (c) Sample Holder, (d) Mask, and (e) OSM Connector

REFERENCES

1. Sobol, H., "Extending IC Technology to Microwave Technology", Electronics, March 20, 1967, p. 112.

2. Assadourian, F., and Rimai, E., "Simplified Theory of Microstrip Transmission Systems", Proc. I.R.E., Vol. 40, December 1952, p. 1651.

3. Kostriza, J. A., "Microstrip Components", Proc. I.R.E., Vol. 40, December 1952, p. 1658.

4. Grieg, D. D., and Engelmann, H. F., "Microstrip -- a New Transmission Technique for the Kilomegacycle Range", Proc. I.R.E., Vol. 40, December 1952, p. 1644.

5. Arditi, M., "Characteristics and Applications of Microstrip for Microwave Wiring", I.R.E. Trans. on Microwave Theory and Techniques, Vol. MTT-3, March 1955, p. 31.

6. Arditi, M., "Experimantal Determination of the Properties of Microstrip Components", Elect. Commun., Vol. 30, 1953, p. 283.

7. Black, K. G., and Higgins, T., "Rigorous Determination of the Parameters of Microstrip Transmission Lines", I.R.E. Trans. on Microwave Theory and Techniques, Vol. MTT-3, March 1955, p. 93.

8. Dukes, J.M.C., "An Investigation of Some Fundamental Properties of Strip Transmission Lines with the Aid of an Electrolytic Tank", Proc. I.E.E. (London), Vol. 103B, 1956, p. 319.

9. Wu, T. T., "Theory of Microstrip", Jour. of App. Phys., Vol. 28, 1957, p. 299.

10. Wheeler, H. A., "Transmission-Line Properties of Parallel Wide Strips by a Conformal Mapping Approximation", I.E.E.E. Trans. Microwave Theory and Techniques, Vol. MTT-12, May 1964, p. 280.

11. Wheeler, H. A., "Transmission-Line Properties of Parallel Strips Separated by a Dielectric Sheet", I.E.E.E. Trans. Microwave Theory and Techniques, Vol. MTT-13, March 1965, p. 172.

12. Caulton, M., Hughes, J. J. and Sobol, H., "Measurements on the Properties of Microstrip Transmission Lines for Microwave Integrated Circuits", R.C.A. Review, Vol. 27, September 1966, p. 377.

13. Seckelmann, R., "Nodal Shift Measurements to Determine Transmission Line Properties", Microwave Jour., Vol. 11, No. 4, April 1968, p. 69.

14. Seckelmann, R., "On Measurements of Microstrip Properties", Microwave Jour., Vol. 11, No. 1, January 1968, p. 61.

15. Hyltin, T. M., "Microstrip Transmission on Semiconductor Dielectrics", I.E.E.E. Trans. Microwave Theory and Techniques, Vol. 13, Nov. 1965, p. 777.

16. Lenzing, H. F., "How to Determine Characteristic Impedance", Elect. Design, May 10, 1963, p. 58.

17. Green, H. E., "The Numerical Solution of Some Important Transmission-Line Problems", I.E.E.E. Trans. on Microwave Theory and Techniques, Vol. 13, September 1965, p. 676.

18. Wolters, K. C., and Clar, P.L., "Microstrip Transmission Lines on High Dielectric Constant Substrates for Hybrid Integrated Circuits", IEEE International Microwave Symposium, Boston, Mass., May 1967, paper V-2.

19. Guckel, H., Brennan, P. A., and Polocz, I., "A Parallel-Plate Waveguide Approach to Microminiaturized Planar Transmission Lines for Integrated Circuits", I.E.E.E. Trans. Microwave Theory and Techniques, Vol. 15, No. 8, August 1967, p. 468.

20. Yamashita, E., and Mittra, R., "Variational Method for the Analysis of Microstrip Lines", I.E.E.E. Trans. Microwave Theory and Techniques, Vol. 16, No. 4, April 1968, p. 251.

21. Smith, R. A., "Semiconductors", Cambridge (1959), p. 162.

22. Collin, R. E., "Field Theory of Guided Waves", New York (1960), McGraw-Hill, p. 162.

23. Montgomery, C. G., Dicke, R. H., and Purcell, E. M., "Principles of Microwave Circuits", Radiation Labs Series, McGraw-Hill (1948), Vol. 8, p. 146.

24. Storer, J. E., Sheingold, L. S., and Stein, S., "A Simple Graphical Analysis of a Two-Port Waveguide Junction", Proc. I.R.E., Vol. 41, August 1953, p. 1004.

25. Deschamps, G. A., "Determination of Reflection Coefficients and Insertion Loss of a Waveguide Junction", Jour. of App. Phys., Vol. 24, August 1953, p. 1046.

26. Champlin, K. S., et al, "Analysis and Calibration of a Reflection Coefficient Bridge for use with any Waveguide Mode", I.E.E.E. Trans. Microwave Theory and Techniques, Vol. 15, August 1967, p. 477.

27. Dynes, R. C., "A Tunneling Investigation of the Mechanisms Determining Superconductivity in Simple Metals and Alloys", Ph.D. thesis, May 1968, p. 71.

28. King, R. W., "Transmission Line Theory", New York: McGraw-Hill Book Co., 1955, p. 282.

29. Valdes, L. B., "Resistivity Measurements on Ge for Transistors", Proc. I.R.E., Vol. 42, 1954, p. 420.

30. Yamashita, E., "Variational Method for the Analysis of Microstrip-Like Transmission Lines", I.E.E.E. Trans. Microwave Theory and Techniques, Vol. MTT-16, August 1968, p. 529.